INVESTIGATION OF JET NOISE USING OPTICAL HOLOGRAPHY

Richard F. Salant
Department of Mechanical Engineering
Massachusetts Institute of Technology
Cambridge, Ma. 02139

JUNE 1972
INTERIM REPORT

Prepared for
U.S. DEPARTMENT OF TRANSPORTATION
OFFICE OF THE SECRETARY
Office of Noise Abatement
Washington D.C. 20590

1. Report No. DOT-TSC-146-1	2. Government Accession No.	3. Recipient's Cotolog No.
4. Title and Subtitle: INVESTIGATION OF JET NOISE USING OPTICAL HOLOGRAPHY		5. Report Date: June 1972 6. Performing Organization Code
7. Author(s): Richard F. Salant		8. Performing Organization Report No.
9. Performing Organization Name and Address: Department of Mechanical Engineering, Massachusetts Institute of Technology, Cambridge, MA 02139		10. Work Unit No. R-2519 11. Contract or Grant No. DOT-TSC-146
12. Sponsoring Agency Name and Address: Office of the Secretary, Office of Noise Abatement, Department of Transportation, Washington, D.C. 20590		13. Type of Report and Period Covered: Interim Report, March 1971 to March 72 14. Sponsoring Agency Code
15. Supplementary Notes		

16. Abstract

Holographic interferograms have been made of a cold, laboratory scale, supersonic jet in the mach number range of 2.1 to 3.4. These holograms demonstrate that the acoustic field in the vincinity of such a jet is dominated by mach waves, each of which can be traced back to a generating disturbance within the jet. The mach waves are generated from an axial position a slightly downstream of the nozzle exit to a position near the tip of the potential core. Measurements of mach angle indicate that the average convection velocity of the generating disturbances is approximately 90% of the jet velocity. The disturbances appear to be coherent instabilities rather than turbulent eddies, and extend into the potential core. Their length scale has a primary peak at from 0.7 to 1.3 jet diameters, and a secondary peak at a somewhat higher wavelength. (These optical measurements are consistent with supplementary microphone measurements.) Accelerometer measurements of nozzle vibration suggest that the generating distrubances originate at, or upstream of, the nozzle.

17. Key Words	18. Distribution Statement
Optical Holography Supersonic Jet Noise Mach waves	DOCUMENT IS AVAILABLE TO THE PUBLIC THROUGH THE NATIONAL TECHNICAL INFORMATION SERVICE, SPRINGFIELD, VIRGINIA 22151.

19. Security Classif. (of this report)	20. Security Classif. (of this page)	21. No. of Pages	22. Price
Unclassified	Unclassified	60	

Preface

This investigation was initiated through grants from the Sloan and Dupont Foundations. Early experiments were performed by Mr. Robert R. Kolesar and Mr. Gregory F. Zaic.

More recently, this research has been sponsored by the Department of Transportation, under DOT Contract TSC-146. The contract monitor was Mr. Raymond Ehrenbeck, DOT Transportation Systems Center. Mr. Jerry Sorrow and Mr. Hisayuki Handa participated in the experimental program.

Some of the results contained in this report have been published in the open literature.[1]

Abstract

Holographic interferograms have been made of a cold, laboratory scale, supersonic jet in the mach number range of 2.1 to 3.4. These holograms demonstrate that the acoustic field in the vicinity of such a jet is dominated by mach waves, each of which can be traced back to a generating disturbance within the jet. The mach waves are generated from an axial position slightly downstream of the nozzle exit to a position near the tip of the potential core. Measurements of mach angle indicate that the average convection velocity of the generating disturbances is approximately 90% of the jet velocity. The disturbances appear to be coherent instabilities rather than turbulent eddies, and extend into the potential core. Their length scale has a primary peak at from 0.7 to 1.3 jet diameters, and a secondary peak at a somewhat higher wavelength. (These optical measurements are consistent with supplementary microphone measurements.) Accelerometer measurements of nozzle vibration suggest that the generating disturbances originate at, or upstream of, the nozzle.

Table of Contents

Tables

Figures

Chapter I. Introduction

A. Supersonic Jet Noise Theory

This report is concerned with cold cylindrical jets which are not only supersonic, but have mach numbers in excess of 2.0. The basic theoretical model for noise generation by such jets was first proposed in 1960 by Phillips[2] and in 1963, in a somewhat different form, by Ffowcs Williams.[3] The latter's analysis is an extension of Lighthill's[4,5] subsonic jet noise theory to the supersonic case.

The above model postulates that the noise producing region of the jet is the turbulent mixing layer, which is viewed as being composed of many eddies, travelling downstream with a range of convection velocities. Some of these eddies travel at velocities which are supersonic relative to the ambient atmosphere, and will therefore carry weak shocks along with them. Phillips has termed these shocks "mach waves." It is a basic postulate of the model that such mach waves are the dominant form of acoustic radiation from the jet.

Using this model, one could predict the acoustic field of the jet, given the turbulent structure of the mixing layer. Lacking such data, Ffowcs Williams has used dimensional arguments to obtain some of the gross characteristics of the acoustic field (similar to Lighthill's treatment of the subsonic jet). Thus, he has found that at large mach numbers, the acoustic intensity should vary as U^3. Agreement of such overall predictions with measured values obtained from rockets, aircraft engines, and laboratory jets, has led to fairly widespread acceptance of the "mach wave theory" by the scientific community.

However, in the last few years a number of investigators have questioned one of the aspects of the above model. While agreeing (for the most part) that mach waves is the dominant form of radiation, these investigators have challenged the thesis that the mach waves are generated by turbulent eddies in the mixing region. They have proposed, instead, that the disturbances generating mach waves are instabilities propagating downstream, through the jet. Some have considered small-scale instabilities confined to the mixing region, while others have studied large-scale instabilities present throughout the jet.

To the author's knowledge, the first instability model for noise generation was proposed by Mamin and Sedel'nikov[6] in 1965, and was discussed in more detail in 1967.[7] These investigators considered the stability of a cylindrical inviscid jet with a "top hat" velocity profile, and found the greatest contribution to the acoustic field comes from the n = 1 instability mode (unsymmetrical mode). The maximum amplification factor for this mode occurs at a Strouhal number between 0.2 and 0.3, which agrees well with experimentally measured peaks in the acoustic spectrum. (Sedel'nikov[8] also analyzed a plane jet, getting somewhat different results.)

This work appears to have been unknown or ignored in the West until 1971, when Liu[9] proposed instability waves in the mixing layer, as a mach wave-generating mechanism. Liu, who was aware of the Russian work and also of the work by Crow[10] on subsonic jets, considered a more realistic velocity profile and the effects of viscosity and superposed turbulence. However, by confining the analysis to the mixing layer, he restricted its applicability to short wavelength disturbances. His

results indicate that the previous inviscid analyses are sufficient to predict such local characteristics as the convection velocity of the disturbances, but more refined analyses (such as his) are necessary to determine the streamwise variations of the disturbances. He computed the streamwise variation of convection velocity and energy.

Subsequent to Liu's work, and apparently unaware of the Russian work, Tam[11] published an instability analysis of an inviscid jet with top hat velocity profile, considering only short wavelength disturbances, which is, in effect, just the short wavelength limit of Sedel'nikov's[7] analysis. His computations of convection velocity appear to agree well with mach angle measurements of short wavelength radiation detected optically near the nozzle of laboratory jets. (See page 4.)

Later in 1971, Bishop, Ffowcs Williams and Smith[12] also expressed support for an instability mechanism. Based on their interpretation of microphone measurements of high speed jet noise, they proposed that the principal noise sources are large-scale wavelike undulations of the jet flow that travel downstream at supersonic speed, and are a result of the instability of the flow.

This emphasis on large-scale instabilities was then carried further by Tam[13] who, in the most recent work on this subject, did a theoretical analysis which revealed that two large-scale unstable waves are preferentially amplified.

While it is not yet possible to decide whether the instability mechanism or the earlier turbulence mechanism provides a better model of the noise generation process, it is important to recognize that proponents of both theories do agree, by and large, that the dominant radiation is in the form of mach waves.

B. Optical Measurements

The above-mentioned postulate concerning the dominance of mach wave radiation was thrown into some doubt, at least for the case of laboratory scale jets, by an experiment reported in 1968. In an attempt to directly verify the dominance of mach waves, Lowson and Ollerhead[14] made shadowgraphs of a mach 2.5 laboratory scale jet. It was expected that a mach wave field would be detected by the shadowgraph. However, the most prominent feature on the photographs is a beam of short wavelength radiation, apparently propagating from the nozzle exit. This nozzle-centered radiation was ascribed by Lowson and Ollerhead to monopole or dipole sources in the turbulent boundary layer of the nozzle. More recent work by Tam (see page 3) however, suggests it is due to an instability in the mixing layer immediately downstream of the nozzle exit. For over- and under-expanded jets, the second-most prominent feature is spherical radiation centered about shock-mixing layer intersection points, presumably the result of shock-turbulence interaction. Finally, approximately fifteen diameters downstream of the nozzle exit, there appear one or two oblique waves which Lowson and Ollerhead identify as mach waves. (These general features are observed on the shadowgraphs of other investigators.[11,15])

From the above results, Lowson and Ollerhead concluded that mach waves play little, if any, role in the acoustic field of laboratory scale jets. However, there is reason to believe such a conclusion is incorrect. In particular, laboratory scale jets are known to obey the U^3 law, which is based on the mach wave model. Thus, the present author believes it is the shadowgraph experiment that is at fault.

As was pointed out by Lowson and Ollerhead, the shadowgraph responds to the second derivative (spatial) of density, rather than the density itself. Therefore, the shadowgraph will emphasize short wavelength radiation over long wavelength radiation, thereby distorting a visualization of a complicated wave field. In particular, it is quite possible that radiation was present in Lowson and Ollerhead's experiment which was stronger than the nozzle-centered radiation, but was undetected because it had too long a wavelength.

There is some evidence to support the above view, in the form of schlieren photographs. Since the schlieren responds to the first derivative of density, it too distorts a wavefield, but not as much as the shadowgraph. A number of schlieren photographs of supersonic jets by early investigators[16,17] unconcerned with noise, are available. Some of these display predominantly nozzle-centered radiation, some predominantly (what appears to be) mach wave radiation, and some both nozzle-centered and mach wave radiation. Love[16] pointed out that the particular form of radiation he recorded depended on how he adjusted the schlieren system. It is therefore clear that the visualizations previously obtained using shadowgraph and schlieren depend very much on the particular optical system used, and not just on the wavefield under study.

This effect was dramatically demonstrated by Jones,[18] who made a shadowgraph and a schlieren of the same jet. The shadowgraph displays only nozzle-cenetered radiation, while the schlieren contained both nozzle-centered and mach wave radiation.

C. The Present Research Program

The above considerations indicate that previous shadowgraph and schlieren photographs do not display a true representation of the acoustic field in the vicinity of a supersonic jet. To obtain such a true representation it is necessary to use an optical system which responds to the density rather than to a derivative of the density.

Thus, the intention of the present program has been to use such an optical system, holographic interferometry, to examine a laboratory scale cold jet, similar to Lowson's and Ollerhead's.[14] The objective of this program has been two-fold. First, to determine the characteristics of the radiated field, in particular the geometry of the dominant radiation and its classification (i.e., mach wave or nozzle-centered). Second, to determine (in so far as possible) the nature of the mechanism generating the radiation. For example, the convection velocities of disturbances generating mach waves can be deduced from measurements of mach angles. Also, it has been expected that one might even be able to directly detect and identify generating disturbances themselves, using the interferometric technique. This cannot, of course, be done with the shadowgraph, or schlieren, because the small-scale turbulent sheath surrounding the jet is so overemphasized that it entirely masks the interior of the jet. It has been hoped that such detection may provide evidence useful in discriminating between the turbulence and instability models of noise generation.

Chapter II. Experimental Apparatus and Procedure[19-22]

A. Holographic Technique

The diagnostic technique used in the present investigation is double-exposure holographic interferometry.[23] It involves making two holograms on the same plate. The first is a transmission hologram of the field of interest (jet in test-section) and the second is a hologram of the ambient field (test section with jet turned off). (The time duration of the first exposure must be short enough to freeze all motion.) When one views the reconstructed double-exposed hologram, one sees an interferogram produced by the interference of the two optical fields, each corresponding to one of the exposures. The opacity of the fringes is proportional to the optical path length change between exposures, and is therefore proportional to the fluid density integrated along the viewing path. Thus, the technique satisfies the requirement stated earlier: it responds to the density rather than a derivative of the density.

This technique has previously been successfully used to visualize shock waves in a ballistic range.[23] A variation of it, time-averaged holography, has been used by the present author[24] and others,[25] to visualize simple acoustic fields.

While the primary advantage of this technique is its sensitivity to density (rather than a derivative), it has additional advantages. First, it has a three-dimensional capability, since the interferogram is recorded and displayed holographically. This allows one, for example, to examine the three-dimensional geometry of wavefronts (see

page 18). Second, precision alignment and precision optical components are unnecessary, unlike conventional interferometry. This is because the two optical fields which form the interferogram pass through the identical optical system, and therefore imperfections in that system tend to cancel out. (For example, a plexiglass test section may be used, while quartz is necessary for conventional interferometry.)

B. Jet Apparatus

A schematic diagram of the experimental apparatus used in the present investigation is contained in Fig. 1, and photographs of the apparatus are in Fig. 2. Two sources of gas were used. For low mach number tests (M = 2.1), a large air compressor was employed. It could deliver 450 ft^3/min at a maximum stagnation pressure of 125 psig. For higher mach numbers (up to M = 3.4), compressed nitrogen was used; three nitrogen cylinders were connected to a manifold feeding the nozzle. With both the air and nitrogen sources, the stagnation pressure immediately upstream of the nozzle was monitored.

Three different converging-diverging nozzles, with circular cross-sections, were used in the experiments; their dimensions are given in Table 1. Nozzle #1 was used for the low mach number air tests. It was machined from steel, with a conical diverging section and a smooth converging section (whose shape was chosen arbitrarily). Nozzle #2 was used for the high mach number nitrogen tests, in which diffuse beam holograms were made. It was cast out of epoxy resin, and was designed with somewhat more care than nozzle #1, to provide a uniform flow across the exit (for details of the contour, see Ref. 26). Nozzle #3, also

cast out of epoxy resin, was used for the high mach number nitrogen tests, in which collimated beam holograms were made. The contour of this nozzle was generated from a "theory of characteristics" algorithim, which had been developed for a plane nozzle, and was rotated about the nozzle axis. All nozzles were used under slightly underexpanded conditions.

The exit velocities of the various jets were determined from stagnation pressure measurements, using one-dimensional isentropic theory, and assuming the stagnation temperature of the jet is equal to the ambient temperature. Since the jets are slightly underexpanded, the significant exit velocity was chosen to be that at the edge of the jet, rather than that in the interior cells.

In all tests, the nozzle exhausted into a rectangular test section, 15" x 16" x 37", constructed of 3/4" plexiglass. The bottom and upstream end walls were lined with acoustic foam to minimize acoustic reflections. (No reflections were detected on any hologram.)

The flow from the test section was removed from the laboratory, by means of an exhaust ducting system fabricated from ventilating ductwork. The initial section of this system was at first lined with high shear fibreglass, to eliminate wave reflections. However, since it was found that even without the fibreglass, reflections could not be detected, in later tests the lining was removed.

C. Holographic Apparatus

The optical system used for making holograms, is shown in Fig. 1. The light source used was an Optics Technology Inc. Model #134 pulsed

ruby laser. This laser is air-cooled, and was used in the Q-switched mode. For the diffuse beam holograms, a dye cell Q-switch was used, while for the collimated beam holograms, a pockels cell was used. With both types of Q-switch, the laser delivers a 20 nanosecond pulse of .5 - 1.0 joules of energy. This energy was periodically measured with a ballistic thermopile. The pulse itself was continuously monitored by a photocell placed near the holographic plate, in order to avoid using occasional multipulses. While the temporal coherence of the laser beam ($\simeq$ 1.0 meter) was sufficient for holography, the spatial coherence was not. To compensate for this, the beam was severely over-expanded, and only the central section used.

As seen from Fig. 1, the optical arrangement used for making holograms, was a conventional side-band transmission system. The mirrors and beamsplitters were of 1.0" diameter, flat to $\lambda/10$, and dielectric-coated because of the high instantaneous powers used. Negative lenses (concave-concave) were used, rather than convex lenses or objectives, also because of the high powers. All optics were mounted by means of standard laboratory mounts and clamps, with the exception of the lenses, which were mounted on micrometer adjusted translation stages. The entire optical system was isolated from the jet-testsection-exhaust duct system, and mounted on a Lansing Model #70.401 air-suspended optical table. The vibration of the table-top was checked by means of a Michelson interferometer, and found sufficiently small to be used for holography. The optical system was made sufficiently rigid by extensive cross-bracing, and the vibration of individual components were checked by means of accelerometers. (While vibration isolation is

not necessary for single-exposures, due to the short exposure time, it is necessary for double-exposures in order to avoid the appearance of extraneous fringes.)

Figure 1 shows a ground glass scattering plate inserted in the object beam, immediately before the test section. This scattering plate was used in making holograms of the low speed air jet, and in one series of holograms of the high speed nitrogen jet, for the purpose of introducing a "three-dimensional effect." The plate scatters rays into a range of directions, so that the reconstructed hologram can be viewed from a range of directions. This allows one to investigate some of the three-dimensional aspects of the acoustic field (see pages 18-19).

In a second series of holograms of the high speed nitrogen jet, the scattering plate was replaced with a collimating system. Since the purpose of this series was to study the jet structure (rather than the acoustic field) it was desired to obtain the highest spatial resolution possible. Such resolution is limited by the ground glass plate, which produces the "speckle effect;" therefore the plate was eliminated. The holograms made using such a system are equivalent to Mach-Zehnder interferograms, and therefore do not have a three-dimensional capability. Thus, the three-dimensional capability was sacrificed to obtain higher spatial resolution.

All holograms were recorded on Agfa Scientia Type 10E75 4" x 5" holographic plates, and processed using standard procedures.

To reconstruct the holograms an Optics Technology Inc. Model #250 c.w. He-Ne laser was used, delivering 15.0 mW of power. (This laser was also used to align the optical system.) A duplicate of the original

reference beam was constructed, using negative lenses, to illuminate the holographic plate. In the case of the diffuse beam holograms, only the virtual image was used for viewing purposes.

The above-mentioned virtual image was photographed using two techniques. In the first, a conventional copy camera with a long focal length lens was placed 15" from the holographic plate (on the viewing side), in order to avoid the zero-order diffracted beam. While this technique yielded satisfactory photographs, it was believed better quality could be obtained by utilizing a larger area of the holographic plate. This was done, in the second technique, by placing a large condenser lens between the camera and the plate, which produced a real image between the lens and the plate. Photographs using both techniques are shown in Figs. 4-6. No striking difference in quality is observed. It is believed that the benefits of using the second technique were offset by the imperfections introduced by the condenser lens. However, it was found that it was easier to adjust the position of the axis of the camera (relative to the hologram) with the second technique than with the first. Thus, the second technique was used for the angular measurements, described on page 19. All photographs were made on Polaroid Type 47 film.

To photograph the images from the collimated beam holograms, it was not necessary to use a camera. The images were directly recorded using a Polaroid film holder, mounted in a light-tight box, far enough away from the plate to avoid the zero-order diffracted beam.

D. Acoustic and Vibration Measurements

To supplement the holographic data, measurements of the acoustic spectra were made using a Bruel and Kjaer Model #4138 1/8" condenser microphone, Model #2615 cathode follower, and Model #2801 power supply. The frequency response of this system is flat to within ± 3dB at 80 KHz. (The frequency range of interest was 5 KHz to 70 KHz.)

Since the range of the spectrum analyzer which was used extends only up to 20 KHz, it was necessary to tape the microphone output at 120 in./sec and play it back at 30 in./sec. The tape recorder used for this purpose was an Ampex Model #FR-1900.

Spectrum analysis was performed using a Federal Scientific Model #UA-14 Ubiquitous real time spectrum analyzer. Although the bandwidth on the analyzer is 50 Hz, due to the difference in tape record and playback speeds, the effective bandwidth was 75 Hz.

In addition to the acoustic spectra measurements, it was found necessary to measure the nozzle vibrations. This was done by means of a Bruel and Kjaer Model #4344 accelerometer. The output of the accelerometer was displayed on an oscilloscope.

Chapter III. Results and Discussion

A. Mach Wave Patterns

A large number of holograms (several hundred) of supersonic jets have been made. Photographs of typical diffuse-beam holograms of the mach 2.1 air jet are shown in Fig. 3. Flow is from left to right. While the nozzle is not visible in these photographs, the position of its exit is indicated. What appears to be the edge of the jet, is actually the edge of the supersonic mixing region, since the density in the subsonic mixing region is too close to atmospheric density to be detected by the interferometer. (Note that the density changes very rapidly near the edge of the supersonic mixing region.[27]) The location of this "edge" agrees well with other investigators' measurements of the supersonic mixing region edge.[28]

It is interesting to note that the interior region of the jet (supersonic mixing region and potential core) is quite visible in these photographs, and details of the density field can be seen. This is in striking contrast to previous schlierens and shadowgraphs, in which the small scale turbulent sheath masks the interior region.

On all three photographs of Fig. 3, oblique lines, emanating from the jet, are visible. It is believed that these lines represent the projections of mach waves. In addition to the fact that the pattern of these lines is what one would expect a mach wave pattern to look like, there is additional evidence to support this view (see pages 18-19).

These three photographs were made from three different holograms of the identical jet under identical conditions (to the limit of the experimenter's control); however, there is some difference in the

radiation patterns detected. The first photograph displays primarily short wavelength radiation, the second primarily long wavelength radiation, and the third both short and long wavelength radiation.

Qualitatively similar holograms were obtained with the high speed nitrogen jet. Some typical photographs of such holograms are shown in Figs. 4-6. Each figure contains two photographs, made using the two photographic techniques described earlier (page 12), of the same hologram.

Through the use of the above-described holograms (and photographs like those in Figs. 3-6) it has been possible to determine the form of the dominant radiation from laboratory-scale supersonic jets (in the mach number regime of interest), one of the primary objectives of the present investigation. Figure 7 contains a schematic diagram of the radiation pattern of the mach 2.1 air jet, which has been constructed from observations of a large number ($\simeq$ 50) of holograms. Qualitatively similar patterns have been observed for the higher mach number nitrogen jet. From this figure (and from the photographs of Figs. 3-6) it is clear that mach waves dominate the radiation field within approximately 15 diameters of the nozzle exit. Neither nozzle-centered nor shock-centered radiation could be detected in any of the holograms. Hence, while the latter radiation is undoubtedly present (since it is detected on shadowgraphs and schlierens), the present results indicate that its intensity is far below that of the mach waves. This conclusion is in agreement with most theories of supersonic jet noise generation, but is in direct contradiction to the conclusions of Lowson and Ollerhead.[14]

From Fig. 7, one can observe a number of features of the mach wave field. For the mach 2.1 air jet, it is noted that mach waves are generated from a point slightly downstream of the nozzle exit to approximately 8 diameters downstream of the exit. It is interesting to observe that the latter downstream limit is quite close to the tip of the potential core. In fact, in the present study mach wave generation was never observed to occur downstream of the core tip. This suggests the possiblity that the potential core may play a role in the generation process. (Another piece of evidence which also suggests such a possibility, is discussed on page 24.) While the upstream limit of the mach wave generation region has not been studied in detail, the observation that it is located somewhat downstream of the nozzle exit is in agreement with the results of Liu.[9]

The observed (from holograms and photographs) geometry of the mach waves are also shown in Fig. 7. Each mach wave, while it is still "attached" to the jet, appears very straight, although there is some variation in mach angle from wave to wave (see page 22). The outer boundary of the mach-wave region is an oblique line originating slightly downstream of the nozzle exit, and inclined at the compliment of the average mach angle to the jet axis. Downstream of the tip of the potential core, the mach waves "separate" from the jet (since there is no longer any generation), and continue to remain straight as they propagate. However, after a few diameters in the direction of propagation, the waves begin to curve, due to diffration.

The fact that each mach wave remains straight during the generating process is somewhat surprising, since it implies that the disturbances

generating the mach waves travel at a substantially constant convection velocity. However, if these disturbances are turbulent eddies, one would expect them to decelerate as they are convected, and therefore generate a curved mach wave (with local mach angle decreasing with distance, along the front, from the jet). Conversely, it is conceivable that instabilities can travel down the jet at substantially constant velocities. Hence,the observations regarding the straightness of the mach waves tend to support the instability theories of mach wave generation.

It should be emphasized that Fig. 7 (and the discussion of that figure) is based primarily on observations of the original holograms rather than on photographs like those in Figs. 3-6. This is because the holograms display mach wave patterns much more prominently and clearly than the photographs, for the following reason. In viewing a hologram, one usually makes continuous changes in the viewing angle. As this is done, more and more mach waves become visible, so that by using a range of viewing angles one can detect a large number of waves on a single hologram, and therefore get a good idea of the form of the radiation pattern. However, in making a photograph, the viewing angle is fixed to one particular value, and therefore only a relatively small number of mach waves are recorded. Hence, the photograph is a rather poor representation of what is on the hologram. The above observation leads to an interesting implication. Since a mach wave will appear most prominent when viewed normal to its axis, the axes of the mach waves must not all be parallel to the jet axis. Thus, the velocities of the generating disturbances are not purely in the axial direction, but

contain transverse components. This is consistent with the theoretical results of Sedel'nikov[7] and Tam.[13]

B. Three-Dimensional Geometry of Mach Waves

Thus far, it has been assumed that the oblique fringes appearing on the holograms represent mach waves, on the basis that the patterns of these fringes generally resemble the patterns expected of mach waves. Additional justification for identifying these fringes as mach waves has been obtained through studying their three-dimensional geometry. According to mach wave theory, the fronts of mach waves should be locally conical. This property can be examined by making use of the three-dimensional capabilities of holography.

If the mach wave fronts are conical and have axes approximately parallel to the jet axis, the density field associated with the mach waves should be locally axisymmetric about the jet axis. For such a field, it can be shown[29] that the fringes of a diffuse beam hologram should focus on a focal plane passing through the jet axis. This has, indeed, been found to be the case (using two methods). First, it can be seen from the photographs of Figs. 3-6 that both the waves and the jet are simultaneously in focus. Second, a camera was adjusted so that the focal plane passed through the jet axis (image) and it was found that this adjustment also yielded the sharpest image of the waves.

While the above considerations demonstrate the locally axisymmetric nature of the (presumed) mach wave density field, they do not yield any additional information regarding the geometry. Such additional information can be obtained by utilizing the variability in viewing

angle of the hologram. Since the holographic interferogram responds to optical path length changes, such response would be greatest for paths tangent to the mach cone. It is therefore resonable to conclude that the fringes which appear on photographs (such as in Figs. 3-6) represent the projections of the mach wave fronts onto the focal plane. Thus, the true mach angle of a wave can only be measured if the optical axis of the camera is normal to the jet axis. If the angle between the camera axis and the normal to the jet axis in increased (above zero), the apparent mach angle (measured from photographs) should increase in a predictable manner. This provides one with a means of verifying if the fringes do indeed correspond to the projections of mach wave fronts. Table 2 summarizes data taken from two holograms in an attempt at such verification. For the first hologram, it was found that the average apparent mach angle increases by 8.7° when the viewing angle is increased by 30°. In the second hologram, it was found the average apparent mach angle increases by 5.3° when the viewing angle increases by 27.4°. While these increases are somewhat higher than those predicted theoretically, they do provide strong support for the assertion that the fringes represent mach waves. The deviations from predicted values may be due to two effects: first, only average mach angles were compared, since it is difficult to identify the same wave in two views; second, in computing the predicted apparent mach angles it was assumed the mach cones had axes parallel to the jet axis, an assumption that has been shown to be weak (see page 17).

C. Convection Velocity Measurements

In order to determine the nature of the disturbances generating mach waves (one of the objectives of this study), it is necessary to measure the convection velocity of such disturbances. This can be done by measuring the mach angles of the resulting waves. For the cases of M = 2.1 and M = 2.7, the mach angles of a large number of waves, on many different holograms, were measured. From these measurements, the convection velocity was determined, noting $V_c/a = \sin^{-1}\theta$. ($V_c \equiv$ convection velocity, $a \equiv$ ambient sound speed, $\theta \equiv$ mach angle.) For each of the above mach numbers, the jet exit velocity (V_j) was determined (using the procedure described on page 9) so that the convection velocities could be expressed as percentages of the jet velocity. This data is contained in Table 3.

The convection velocities of all waves, detected at each mach number, were averaged to obtain an average convection velocity. (This averaging was done without respect to wave location.) These results are displayed in Table 4. It can be seen that the average convection velocities measured at M = 2.1 and 2.7 are, respectively, $0.87V_j$ and $0.90V_j$. Thus, the significant increase in mach number (31%), results in very little change in V_c/V_j (3.5%).

The comparative insensitivity of V_c/V_j to mach number, however, is not as surprising as the magnitudes of the measured V_c/V_j, which are somewhat higher than expected. In early theoretical work,[3] it had been assumed $V_c/V_j \simeq 0.5$. This value was obtained by assuming the disturbances are confined to the mixing layer, which was modeled as an infinitesimally thin vortex sheet (a very poor model). It is important

to note that the 50% figure has never been verified experimentally, although for subsonic jets hot wire measurements have been made. These indicate that the convection velocity is approximately $0.6V_j$, in the region of highest turbulence intensity.[30] However, the present author believes one is not justified in extrapolating such low mach number results to the supersonic case.

The only convection velocity measurements for supersonic jets, which the present author is aware of, were made optically. Tam's[11] mach angle measurements from shadowgraphs yield convection velocities of approximately $0.75V_j$, a figure lower than those obtained in the present investigation. However, Tam's measurements were for nozzle-centered waves, which are not of interest in the present investigation, and therefore do not cast doubt on the present results. Similarly, Lowson and Ollerhead[14] obtained convection velocities of $0.82V_j$ - $0.86V_j$ for nozzle-centered waves. However, Lowson and Ollerhead also measured V_c for the one or two suspected mach waves which they detected, and obtained a value of $0.90V_j$. This is consistent with the present results (although the close correspondence is probably fortuitous, because of the significant spread in convection velocity and the sparseness of Lowson's and Ollerhead's data).

In summary, previous measurements of convection velocity do not cast doubt on the present measurements (and, in one instance, supports them). The latter indicate that the average convection velocity for supersonic jets (in the mach number range of interest) is substantially higher than would be expected from subsonic jet measurements.

In addition to considering average convection velocities, it is instructive to examine the convection velocities of individual waves. From Table 3, it is seen that these can differ substantially from the average V_c. In fact, extremely high convection velocities, higher than the jet velocity, exist. This result is quite surprising, and would not be possible if the generating disturbances are turbulent eddies. Thus, it is believed that this result supports the view that the disturbances are instabilities.

The spreads in convection velocity, implied above, are recorded in Table 4. It is seen that at M = 2.1, the spread is a comparatively small 14%, and all the mach waves are effectively parallel. However, an increase in mach number to 2.7, results in an increase in spread to 43%. This rather large increase in spread is particularly striking when compared to the small change in V_c/V_j described earlier. However, it is consistent with instability theory.[7]

The preceding discussions of convection velocity have not taken account of wave location. In an attempt to determine the axial variation in V_c, mach angle measurements were made as a function of axial location on two holograms of the M = 2.7 jet. The results are shown in Fig. 8. Within the scatter of the measurements, it appears that V_c remains constant over approximately the first four diameters of the jet. However, this conclusion must be viewed as highly tentative since, in order to accurately determine the axial variation in V_c, it is necessary to obtain statistical data from a large number of holograms.

D. Generating Disturbances

Since mach waves have been identified as the principal form of acoustic radiation emitted by the jets under study, it is important to identify the physical mechanism responsible for their generation. While a complete identification is a major task, beyond the scope of the present investigation, it is believed this investigation has revealed a number of important characteristics of the mechanism. (one particular characteristic, the convection velocity of the generating disturbances, has already been discussed.)

In the photographs of Figs. 3-6, most of the mach waves can be traced back to disturbances in the jet, which are manifested as ripples in the fringe pattern. This is especially evident in the second photograph of Fig. 3, where each mach wave can clearly be traced back to a large undulation in the jet. The overall pattern is strikingly similar to the density field produced by supersonic flow over a wavy wall. It is believed that these photographs show the link between jet disturbances and emitted radiation more directly than any other experiment, thus far. The disturbances, moreover, have the appearance of a coherent instability, rather than that of a turbulent eddy, providing additional support for the instability model of jet noise generation.

In order to obtain a more detailed view of the jet disturbances, an enlargement of a region near the jet where a mach wave appears to originate, was made and is shown in Fig. 9. The mach wave and associated disturbance are quite clear, and are labelled. Also shown on the photograph is the location of the potential core, which was

determined from experimental measurements of another investigator.[17] From this photograph it is clear that the disturbance is not confined to the mixing layer, as has been assumed by proponents of the turbulence model[2,3] and even some supporters of the instability model.[9] It is seen to extend into the potential core, and may even originate in that region. This would be consistent with the observation that mach waves are not generated downstream of the tip of the potential core.

An attempt to obtain further information regarding the disturbances was made, by taking a series of collimated beam holograms of the jet (using nozzle #3) at mach numbers ranging from 2.7 to 3.4 with 0.1 intervals. As discussed earlier (page 11), it was reasoned that such holograms would result in better resolution of the jet flow field than that obtained in the diffuse beam holograms, because of elimination of the speckle effect. A composite photograph of typical holograms of the M = 2.9 jet is shown in Fig. 10. (Holograms at the other mach numbers are qualitatively similar.) From this photograph it can be seen that higher resolution was indeed achieved, since smaller scale features are visible which are not present on the diffuse beam photographs. However, the most prominent features of this photograph are the large scale undulations of the jet. As was mentioned earlier, it is believed that it is these undulations which represent the mach wave-generating disturbances.

To properly analyze these undulations it is necessary to Fourier analyze the various fringes within the jet. However, since the necessary equipment to do this was not available, a cruder analysis was performed. For each photograph, the next to the last visible fringe on either side

of the jet was traced, and coherent disturbances were identified. The peak to peak wavelength of each such disturbance was then measured. This was done for a large number of holograms at each mach number, so that typically 35 disturbances were considered at each mach number. From this data, wavelength spectra, with a bandwidth of 0.2", were constructed. These are contained in Figs. 11-18.

From the above figures, it is seen that all spectra contain primary peaks, and some contain secondary peaks. Except for the spectrum at M = 2.7, it appears that the steepness of the peaks increases with increasing mach number.

The peak wavelengths, for both the primary and secondary peaks, are plotted as a function of mach number in Fig. 19. As seen from this figure, the primary peak wavelength ranges from 0.5" to 0.9", corresponding to λ/D ranging from 0.7 to 1.3 . (The variation is believed to be of the order of the scatter of the data reduction technique.) The secondary peaks always occur at wavelengths larger than the primary wavelength, except for the M = 3.0 case.

From photographs like that in Fig. 10, it appears that the short wavelengths occur throughout the jet, while the long wavelengths occur primarily in the downstream region. Thus, it was hypothesized that the secondary peak is associated with the downstream region. This hypothesis has been examined by plotting the wavelength of each disturbance as a function of the axial location of the disturbance. Such a plot, for M = 2.7, is contained in Fig. 20. It is seen that for axial positions less than 4", the disturbances cluster about a wavelength of approximately 0.7". However, at positions above 4", the disturbances break into two

branches, the lower branch corresponding to the primary peak and the upper branch corresponding to the secondary peak. While there is a great deal of scatter in this data, it is believed that it supports the above-mentioned hypothesis.

E. Acoustic Measurements

All of the experimental results of this investigation, reported thus far, have been based on optical measurements. Such measurements recorded the instantaneous density field, and hence, no direct evidence of the propagation of the oblique fringes (representing mach waves) has been presented. While it is believed sufficient evidence has been presented to establish that the detected oblique fringes do represent mach waves, and therefore must propagate, it was judged necessary to supplement the instantaneous optical measurements with time-dependent acoustic measurements.

For the above purpose, a microphone was placed 4" downstream of the exit of nozzle #3, and 2" radially displaced from the nozzle axis. This location was chosen so as to detect primarily waves generated by disturbances near the primary wavelength peak. The above microphone was used to record acoustic spectra at mach numbers ranging from 2.7 to 3.2, which are contained in Figs. 21-25.

All of these spectra contain peaks at frequencies ranging from 33KHz to 34KHz, with the frequency (slightly) increasing with increasing M. The disturbance wavelengths corresponding to these frequencies have been computed by assuming the propagation speed of the disturbances is 90% of the jet velocity, on the basis of the mach angle measurements

discussed earlier. Such computations, yield disturbance wavelengths ranging from 0.63" (M = 2.7) to 0.65" (M = 3.2). From Fig. 19, it is seen these values fall within the range of primary peak wavelengths recorded optically. Thus, these results indicate that the jet disturbances and associated mach waves which have been detected optically are responsible for the acoustic signals detected by the microphone.

It can also be seen from Figs. 21-25 that the peak in the acoustic spectrum becomes more pronounced as the mach number is increased. This is consistent with similar observations of the optically measured disturbance spectra, described on page 25, further strengthening the correlation between optical and acoustic measurements.

F. Vibration Measurements

Since the results discussed thus far indicate that the acoustic field, consisting primarily of mach waves, is generated by detectable disturbances in the jet which are likely to be coherent instabilities, it is of interest to determine the location of the region in which these disturbances originate. For this purpose, measurements of the nozzle vibrations, using an accelerometer, were made at a mach number of 2.8. A typical oscilloscope trace of these vibrations is contained in Fig. 26, and indicates the vibration amplitude is quite small, less than 1 micron (less than 10^{-6}% of the nozzle diameter). However, it is interesting to note that the dominant frequency is 32 KHz. This corresponds, effectively, to the peak in the acoustic spectrum, indicating correlation between the nozzle vibrations and the acoustic field.

(The slight discrepancy between the peaks of the two types of spectra may be due to the fact that the jet was removed from the test section during the vibration measurements.)

The above-mentioned correlation might be due to one of three possible effects. It may be argued that the correlation occurs because acoustic waves propagate back to the nozzle, causing it to vibrate. However, it should be noted that in spite of the small vibration amplitudes, the peak accelerations are quite large, due to the high frequencies. To produce such accelerations would require very large amplitude acoustic waves propagating towards the nozzle, which are not detected on the holograms.

There remain two additional hypothese to explain the results. First, it is the vibration of the nozzle itself, which triggers the instability that eventually generates the mach waves. This hypothesis will shortly be tested by a series of experiments to be reported elsewhere. However, it should be pointed out that at the present time this hypothesis appears unlikely, because of the small amplitude of the nozzle vibrations. If such vibrations do trigger the instability, an extremely large amplification rate would be necessary.

A second possible hypothesis follows: fluctuations in the flow field upstream of the nozzle exit both trigger the instability and cause the nozzle to vibrate. The detailed characteristics of these fluctuations would be determined by the flow apparatus upstream of the nozzle.

Regardless of which of the above two possible hypotheses is correct (or even if another unknown mechanism is responsible), it is

reasonably certain that the disturbances which generate the mach waves originate at, or upstream of, the nozzle. Thus, these results strongly support the instability model of the generation of supersonic jet noise.

Chapter IV. Future Work

Future work, under the present contract, will be concentrated in three major areas:

A. Holographic Study of Cold Jet Noise

Additional details of the cold jet noise field will be obtained using the techniques developed during the present program. In particular, the distribution function for convection velocity will be obtained as a function of mach number, by means of holographic observations. Additional data on the variation of convection velocity with axial position will also be obtained.

In the present report, wavelength spectra obtained from disturbance measurements have been described. To supplement this data, attempts will be made to obtain the wavelength spectra from holographic measurements of the acoustic field.

The above measurements will be compared, in so far as possible, with the predictions of various analytical models.

In addition, the detailed structure of the mach-wave-generating disturbances will be further examined, holographically. Efforts to determine the precise lateral and axial positions of the disturbances, will be continued.

B. Nozzle Vibration Study

Results described in this report suggest the possibility of a link between nozzle vibrations and the noise generation process. To investigate such a link, and the role of instabilities in the noise generation process, an experiment will be performed in which a nozzle

will be vibrated by means of an external signal. A special nozzle has been constructed, in which an annular nozzle extension has been formed from a piezoelectric crystal. An oscillating voltage is applied to this crystal by means of an oscillator (and associated electronics), which causes the extension to vibrate in the radial direction. Such vibrations will be set up for a range of frequencies and jet conditions, and their effects on the acoustic spectrum and jet structure will be measured.

C. Helium Jet Study

A scaling analysis has indicated that the present experimental apparatus can be used to simulate hot jet noise, if a light test gas is used. For this purpose, a large number of holograms will be made of a helium jet, under a variety of conditions. Emphasis will be placed on detecting and identifying phenomena not present in the air and nitrogen jet experiments, if such phenomena do indeed occur.

Chapter V. Conclusions

The results of the present investigation, reported in the preceding chapter, lead to the following principal conclusions:

1. The acoustic field in the vicinity of a cold, laboratory scale, supersonic jet in the mach number range of 2.1 - 3.4, is dominated by mach wave radiation.

   This conclusion, based on observations of several hundred holograms, directly contradicts the conclusion of Lowson and Ollerhead, but agrees with most theoretical models of supersonic jet noise generation. It is believed that the shadowgraph technique, used by Lowson and Ollerhead, distorts the acoustic field and therefore had led to a faulty conclusion.

   This direct experimental verification of the dominance of mach wave radiation should contribute towards providing a sound base for further research on the fundamental noise generation process in supersonic jets.

2. The mach waves are generated by jet disturbances which travel downstream with convection velocities of approximately 90% of the jet velocity.

   This conclusion is based on mach angle measurements of a large number of waves, and is somewhat surprising since it is known that in subsonic jets the average convection velocity is approximately 60% of the jet velocity. However, since no data have been found which contradict the present results, it is believed that these results suggest a qualitative difference between the noise generating disturbances in supersonic and subsonic jets.

3. The mach waves are not generated downstream of the potential core.

This conclusion is based on observations of a large number of holograms, and suggests the possibility that the potential core may play a role in the noise generation process. It is consistent with several recent instability models of the noise generation process.

4. The jet disturbances are not confined to the mixing layer, but extend into the potential core.

This conclusion is based on visual observations of disturbances detected on holograms, and again suggests the possibility that the potential core may play a role in the noise generation process. It should be noted that this conclusion contradicts the traditional turbulence model of noise generation, but is consistent with the more recent instability models.

5. The disturbance length scale has a primary peak between 0.7 and 1.3 jet diameters, and a secondary peak at a somewhat longer wavelength.

This conclusion is based on wavelength spectra which have been constructed from observations of a large number of disturbances on collimated beam holograms. The conclusion is not surprising, and is consistent with most theories of jet noise.

6. The disturbances have the appearance of coherent instabilities, rather than turbulent eddies.

This conclusion is based on visual observations of disturbances on several holograms, on the observation that some disturbances have convection velocities which exceed the jet velocity, and on the evidence cited under items #2 - #4. This conclusion supports the recent instability models of jet noise generation.

7. The disturbances originate at, or upstream of, the nozzle.

This conclusion is based on a limited number of comparisons between the nozzle vibrations and the acoustic field. Hence, this conclusion must be viewed as tentative, subject to further investigation. However, it has important implications in regard to possible measures for the alteration and control of the acoustic field.

References

1. Salant, R. F., Zaic, G. F., Kolesar, R. R., Proc. Purdue Conf. on Noise Control, 444, Purdue U. Press, Lafayette, (1971).

2. Phillips, O. M., J. Fld. Mech., 9, 1, (1960).

3. Ffowcs Williams, J. E., Phil. Trans. Roy. Soc. A, 255, 469, (1963).

4. Lighthill, M. J., Proc. Roy. Soc. A, 211, 564, (1952).

5. Lighthill, M. J., Proc. Roy. Soc. A, 222, 1, (1954).

6. Mamin, V. M., Sedel'nikov, T. Kh., Sov. Phys.-Acous., 11, 255, (1965).

7. Sedel'nikov, T. Kh., NASA TT F-538, 71, (1967).

8. Sedel'nikov, T. Kh., NASA TT F-538, 76, (1967).

9. Liu, J. T. C., AIAA Preprint 71-150, (1971).

10. Crow, S. C., Champagne, F. H., J. Fld. Mech., 48, 547, (1971).

11. Tam, C. K. W., J. Fld. Mech., 46, 757, (1971).

12. Bishop, K. A., Ffowcs Williams, J. E., Smith, W., J. Fld. Mech., 50, 21, (1971).

13. Tam, C. K. W., J. Fld. Mech., 51, 69, (1972).

14. Lowson, M. V., Ollerhead, J. B., J. Acous. Soc. Am., 44, 624, (1968).

15. Dosanjh, D. S., Yu, J. C., in Aerodynamic Noise (H. S. Ribner, Ed.), 169, U. Toronto Press, Toronto, (1969).

16. Love, E. S., et al., NASA TR R-6, (1959).

17. Eggers, J. M., NASA TN D-3601, (1966).

18. Jones, I. S. F., AIAA Preprint 71-151, (1971).

19. Kolesar, R. R., S. M. Thesis, Dept. of M. E., M. I. T., (1971).

20. Zaic, G. F., S. M. Thesis, Dept. of M. E., M. I. T., (1971).

21. Sorrow, J., S. M. Thesis, Dept. of M. E., M. I. T., in prep.

22. Handa, H., Sc.D. Thesis, Dept. of M. E., M. I. T., in prep.

23. Witte, A. B., Wuerker, R. F., AIAA Preprint 69-347, (1969).

24. Salant, R. F., et al., J. Acous. Soc. Am., 44, 1732, (1969).

25. Belogorodskii, B. A., et al., Sov. Phys.-Acous., 17, 303, (1971).

26. Rosales, A. A., S. M. Thesis, Dept. of Aero. and Astro., M. I. T., (1970).

27. Godderum, P. B., et al., NACA Rept. 963, (1950).

28. Nagamatsu, H. T., Sheer, R. E., Horvay, G., in NASA SP-207, 17, (1969).

29. Heflinger, L. O., Wuerker, R. F., Brooks, R. E., J. Appd. Phys., 37, 642, (1966).

30. Davies, P. O. A. L., Ko, N. W. M., Bose, B., Aero. Res. Counc. Rept. CP No. 989, (1967).

Nozzle #	Throat Diameter	Exit Diameter	Design Mach Number
1	0.500"	0.634"	1.94
2	0.276"	0.455"	2.54
3	0.300"	0.690"	3.24

Table 1. Nozzle Dimensions

	Average Original Mach Angle	Viewing Angle	Average Apparent Mach Angle (Measured)	Average Apparent Mach Angle (Predicted)
Hologram #1	41.1°	30.0°	49.8°	45.3°
Hologram #2	40.2°	27.4°	45.5°	43.6°

Table 2. Variable Viewing Angle Measurements, M = 2.7

M = 2.1 (Air Jet)	M = 2.7 (Nitrogen Jet)	
85.1	112.6	75.2
82.6	101.9	90.9
87.0	109.8	89.1
86.6	97.4	74.1
86.8	98.1	77.9
92.4	95.1	85.7
83.4	78.1	80.8
87.0	75.4	103.8
89.7	79.6	108.0
81.3	90.5	106.6
89.7	76.6	101.2
87.0	77.5	86.4
	84.1	76.8

Table 3. Measured Disturbance Convection Velocities (as percent of jet velocity)

Jet Mach Number	Average Convection Velocity	Spread in Convection Velocity
2.1	0.87 V_j	14%
2.7	0.90 V_j	43%

Table 4. Summary of Convection Velocity Measurements

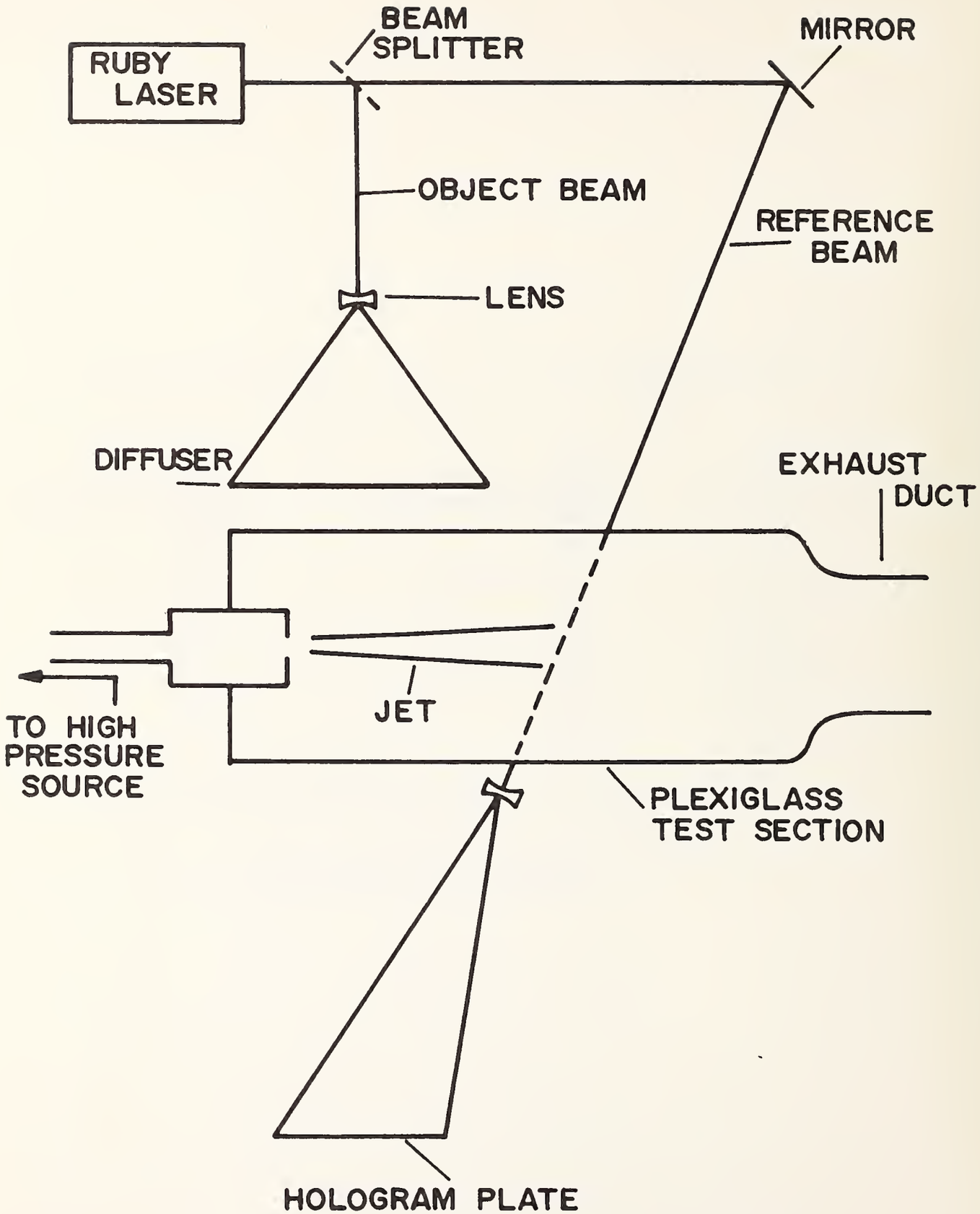

Figure 1a. Schematic Diagram of Experimental Apparatus for Diffuse Beam Holograms

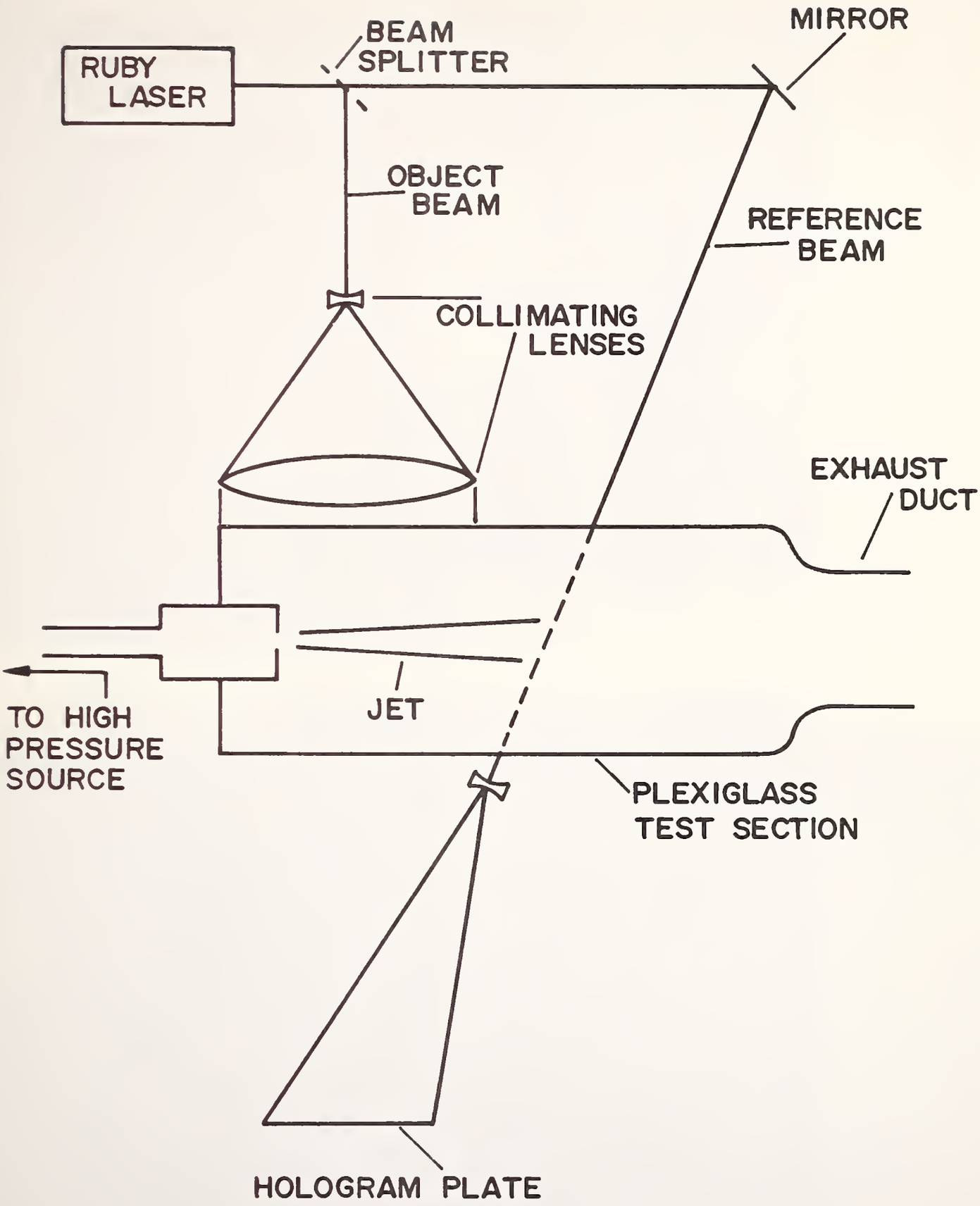

Figure 1b. Schematic Diagram of Experimental Apparatus for Collimated Beam Holograms

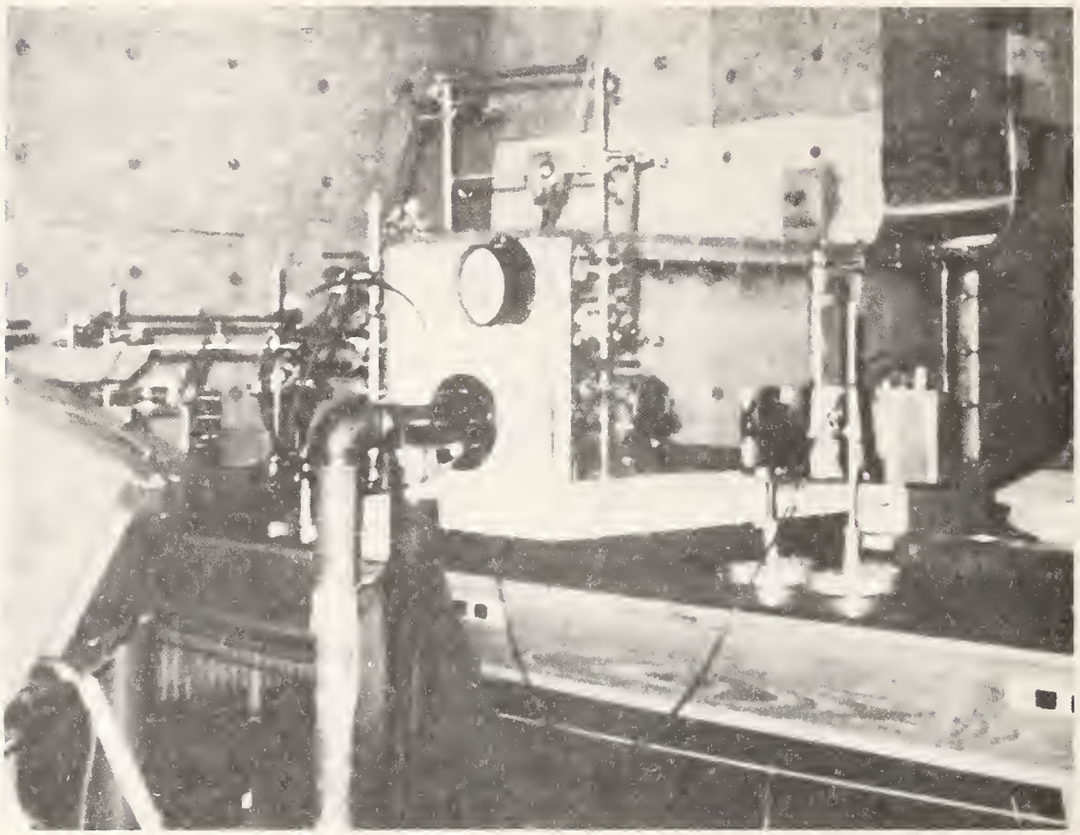

With Air Jet

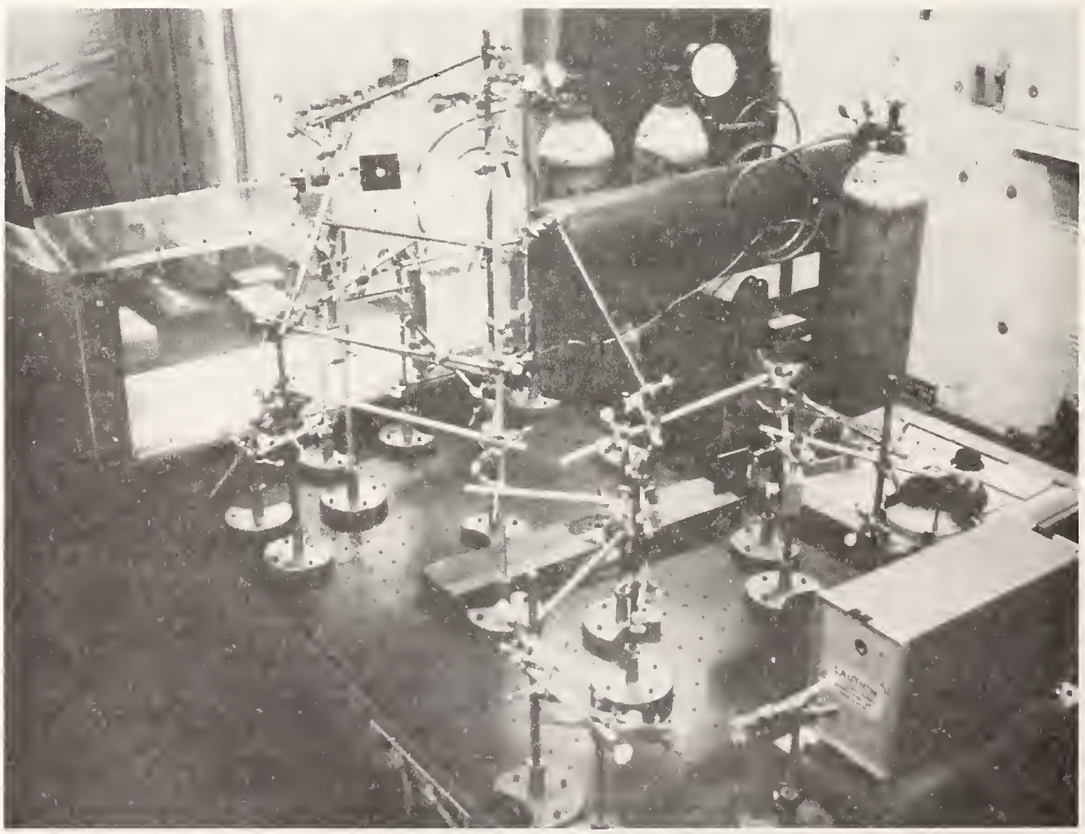

With Nitrogen Jet

Figure 2. Photographs of Experimental Apparatus

3a

3b

3c

Figure 3. Holograms of M = 2.1 Jet

Virtual Images

Virtual Image

"Real Image"

Figure 4. Hologram of M = 2.7 Jet

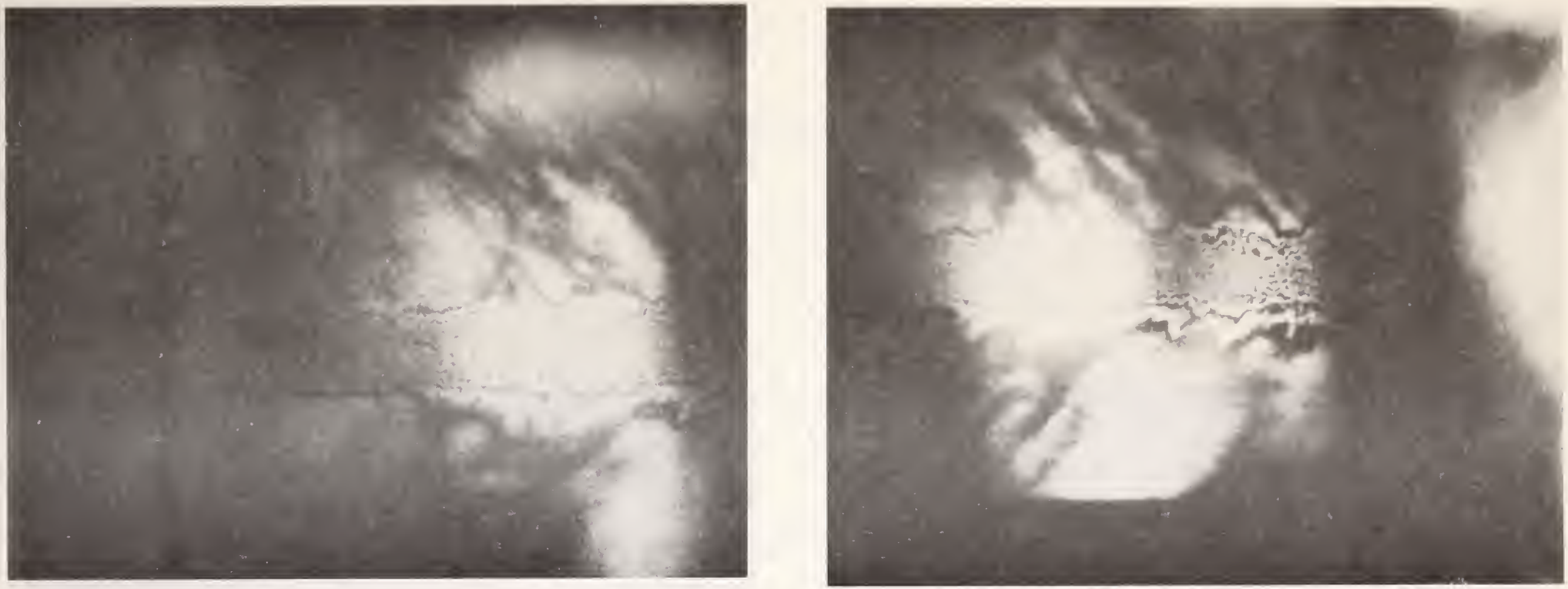

Virtual Image

"Real Image"

Figure 5. Hologram of M = 2.7 Jet

Virtual Image

"Real Image"

Figure 6. Hologram of M = 2.7 Jet

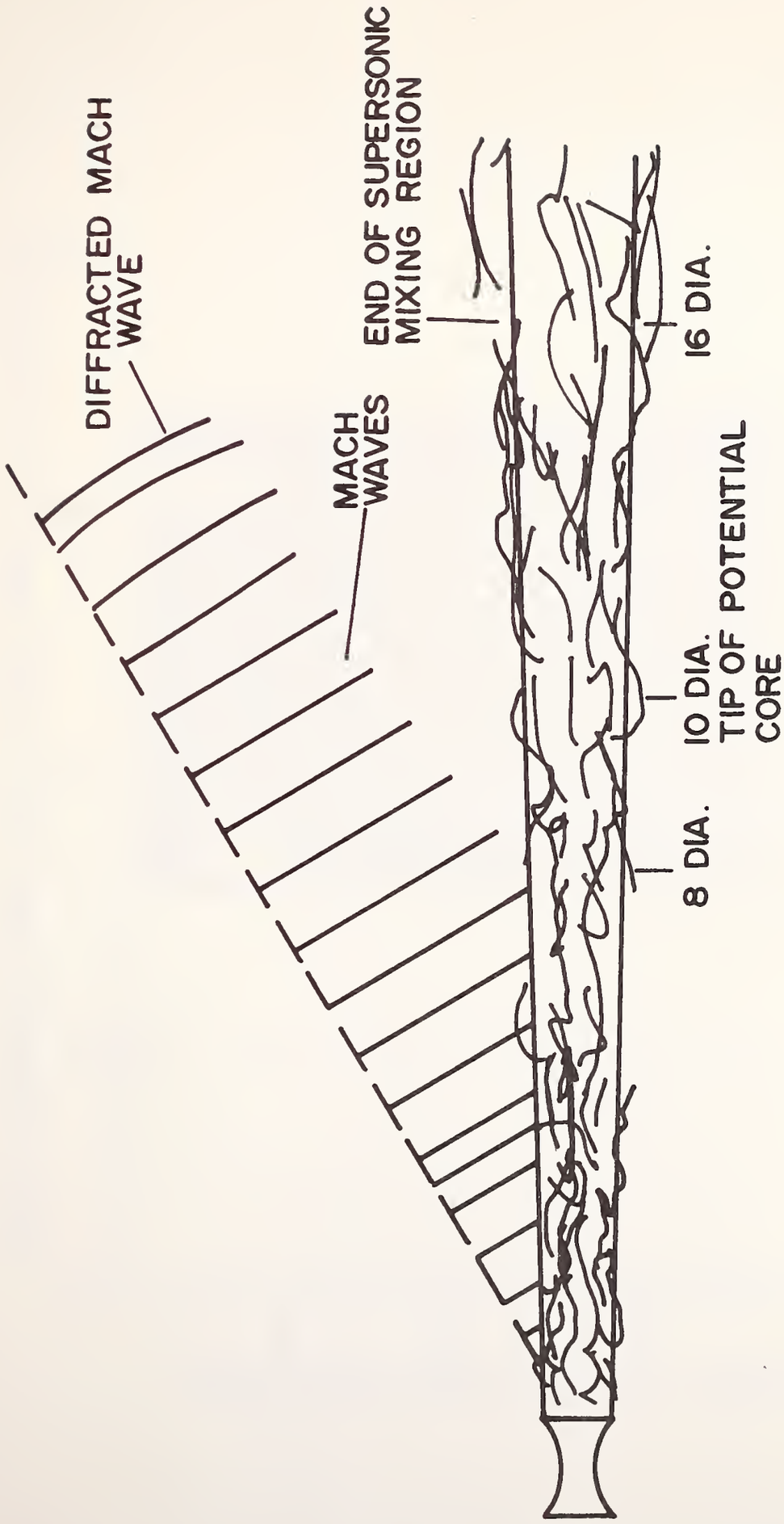

Figure 7. Schematic Diagram of Radiation Pattern of M = 2.1 Jet

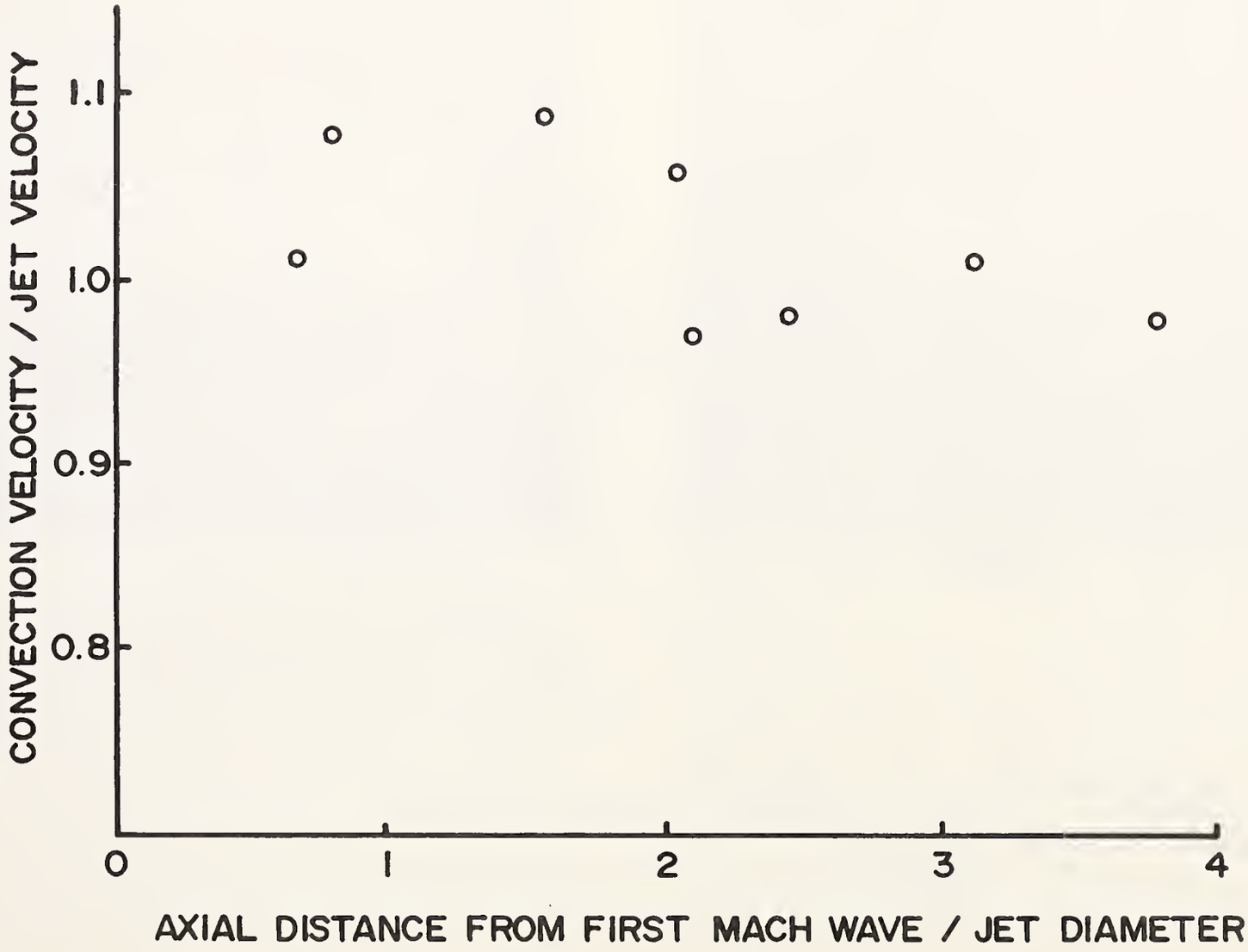

Figure 8. Axial Variation in Convection Velocity, M = 2.7 Jet

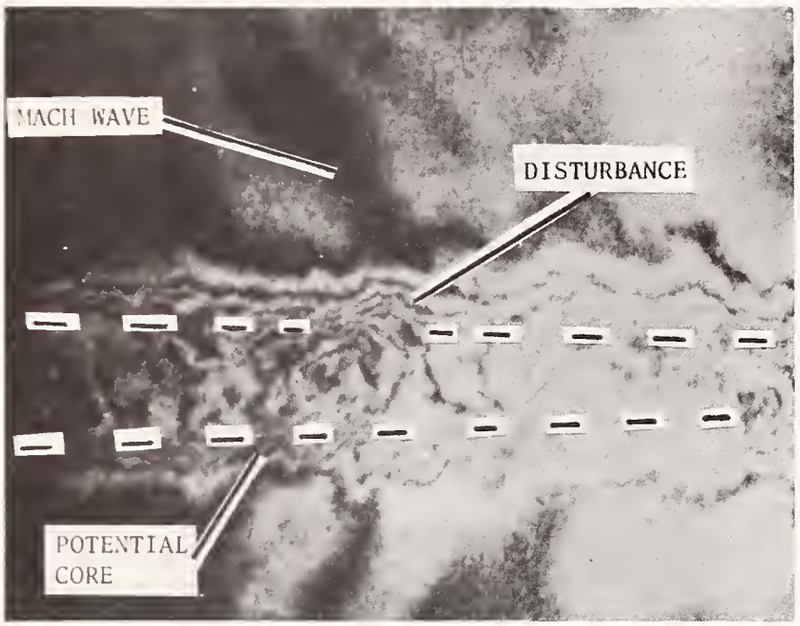

Figure 9. Detailed View of Jet Disturbance, M = 2.1

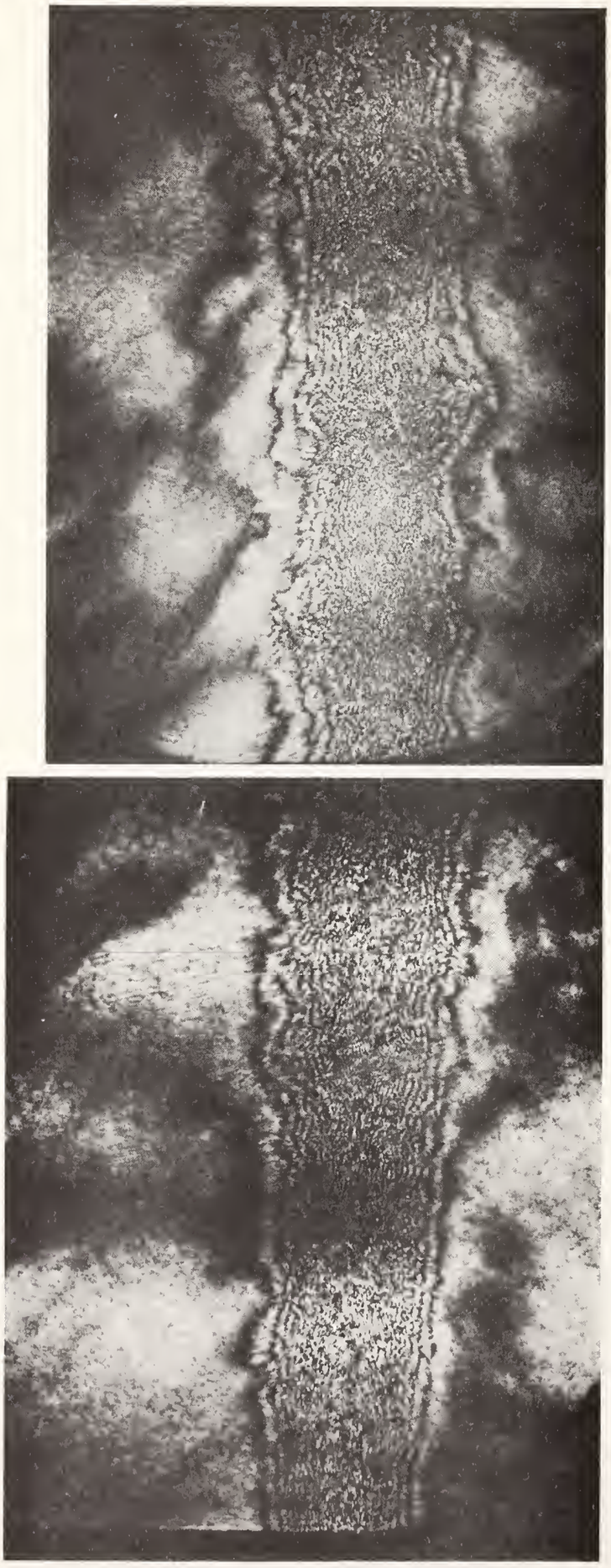

Figure 10. Collimated Beam Hologram of M = 2.9 Jet

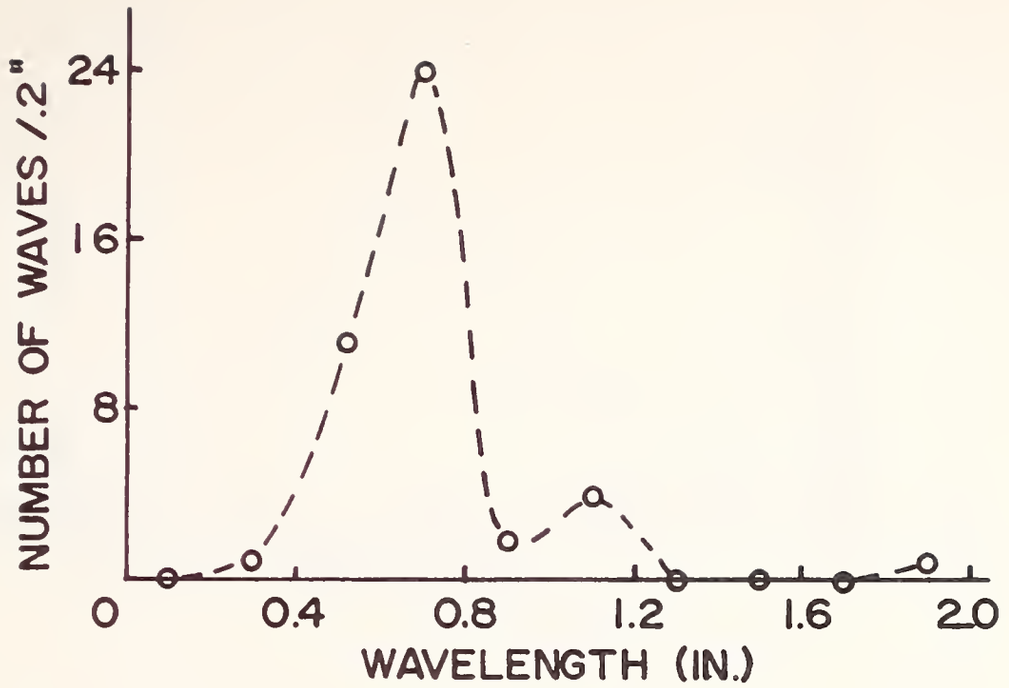

Figure 11. Disturbance Spectrum, M = 2.7

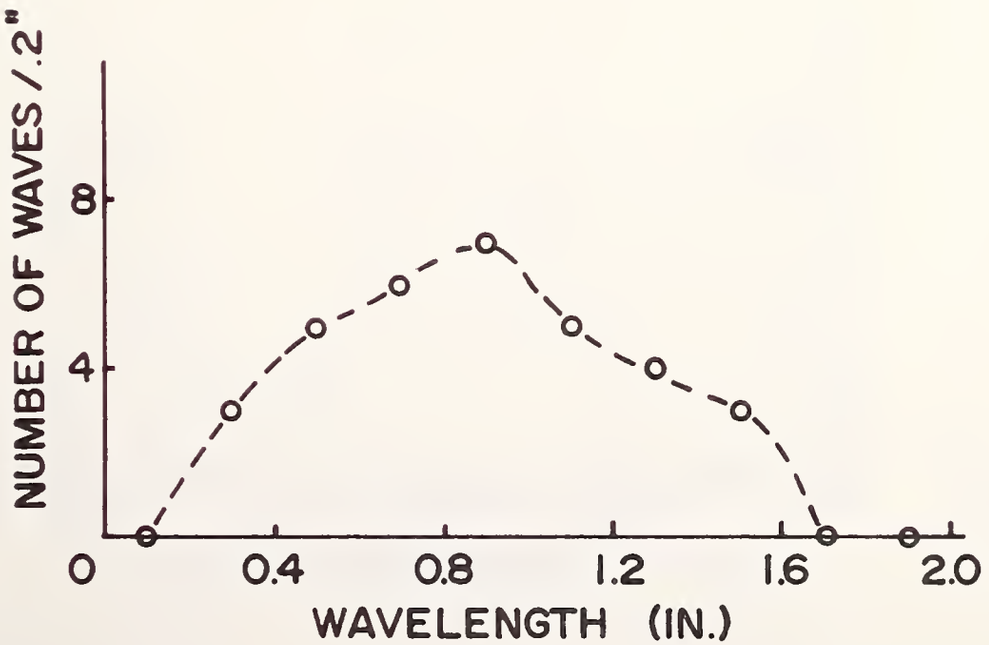

Figure 12. Disturbance Spectrum, M = 2.8

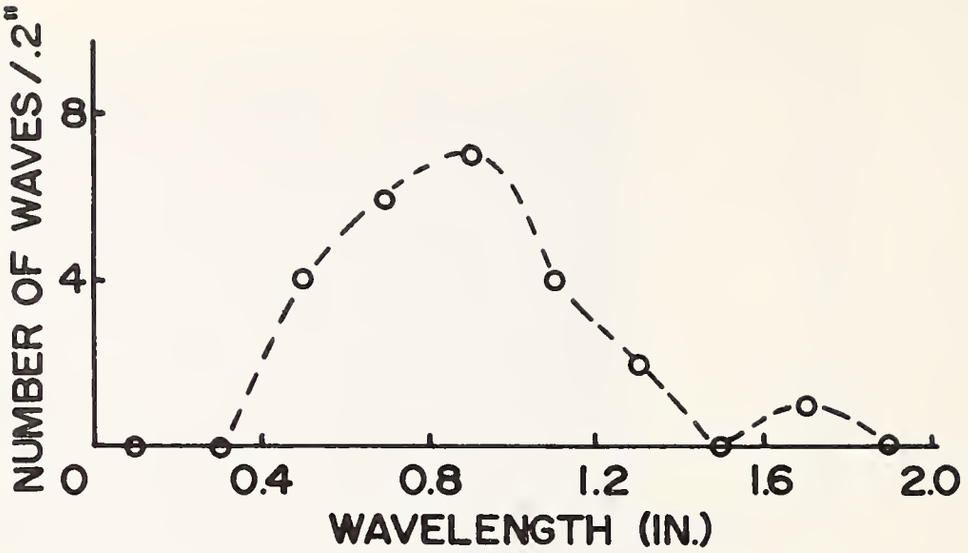

Figure 13. Disturbance Spectrum, M = 2.9

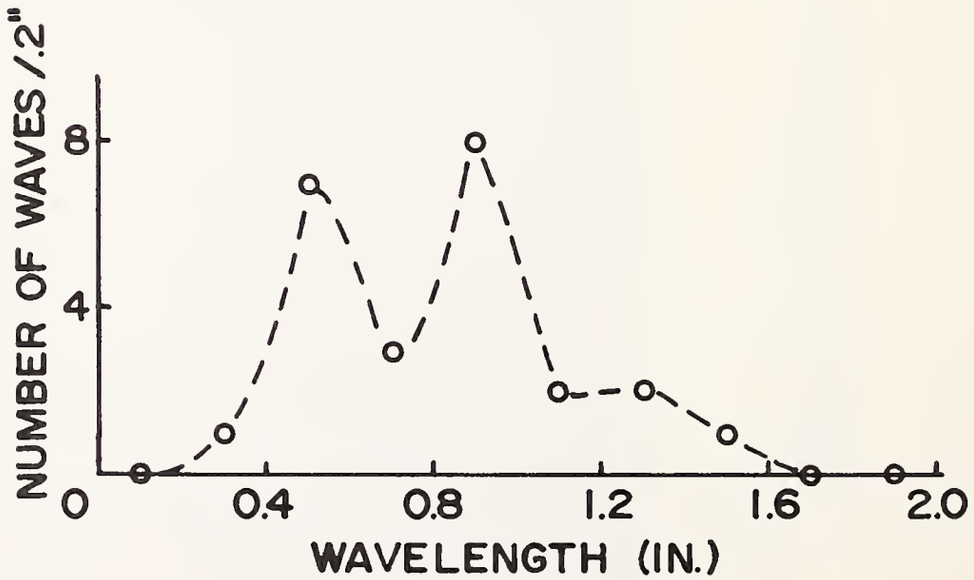

Figure 14. Disturbance Spectrum, M = 3.0

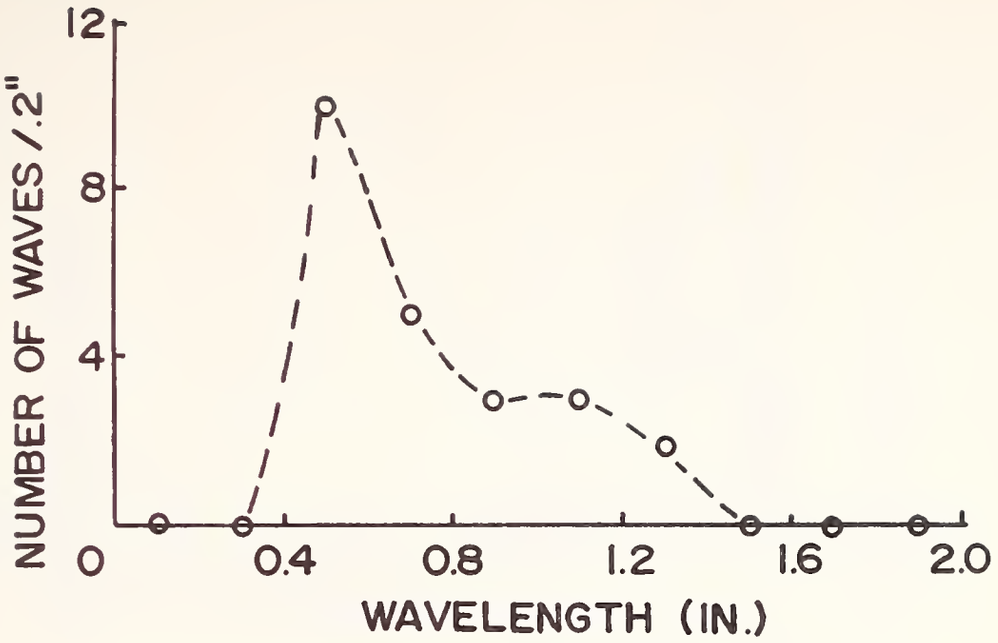

Figure 15. Disturbance Spectrum, M = 3.1

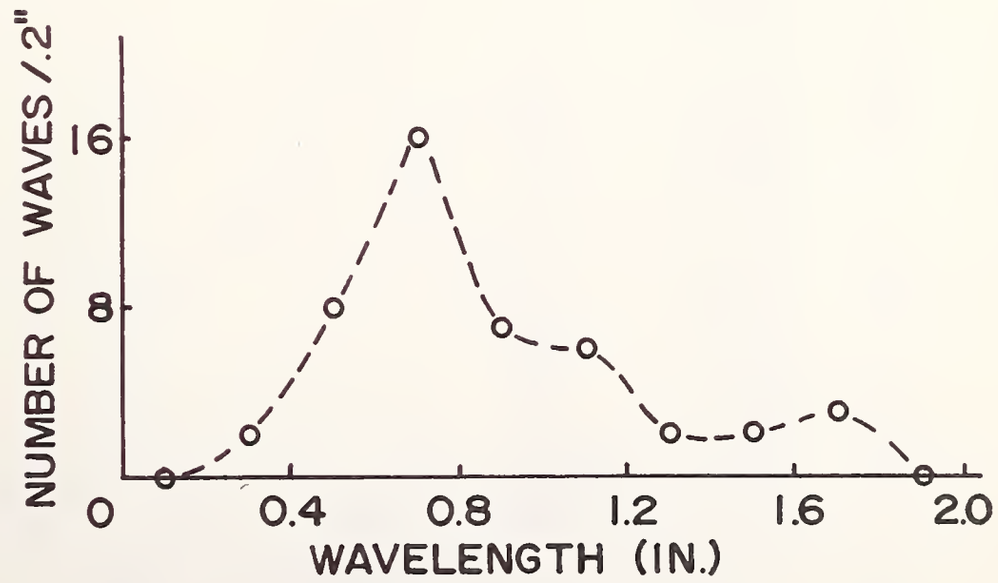

Figure 16. Disturbance Spectrum, M = 3.2

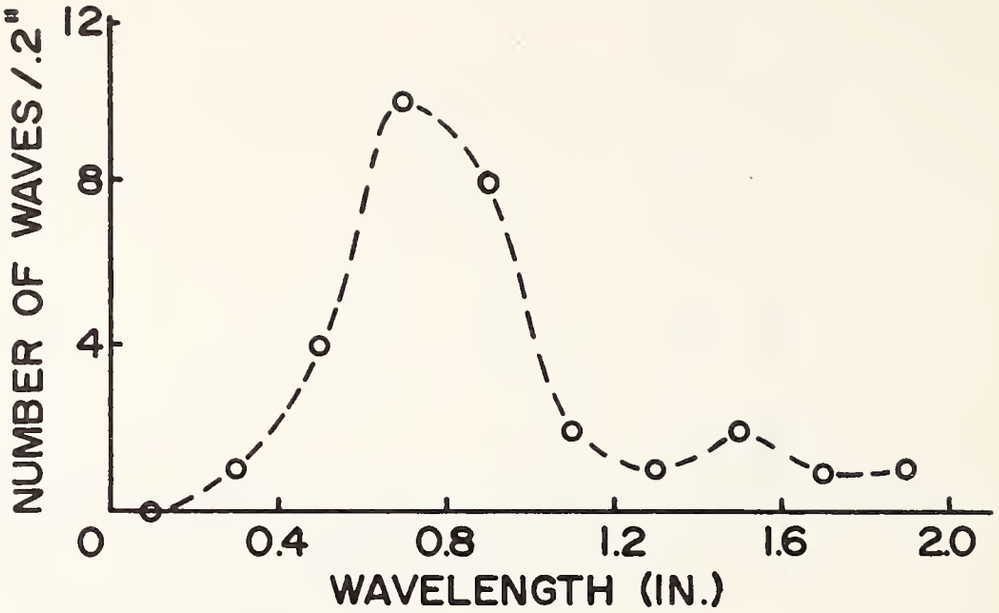

Figure 17. Disturbance Spectrum, M = 3.3

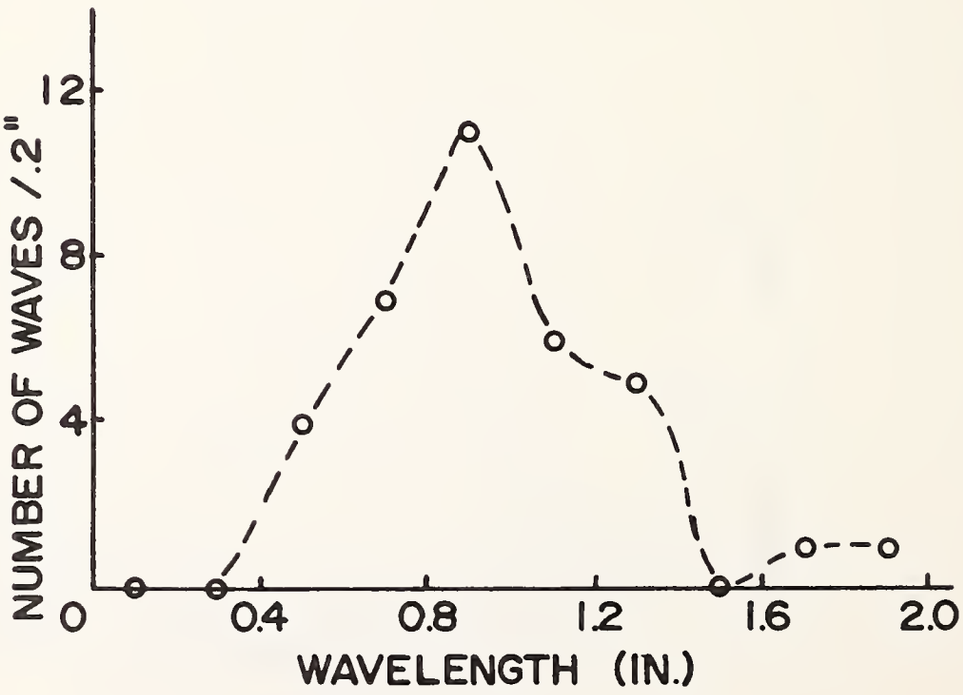

Figure 18. Disturbance Spectrum, M = 3.4

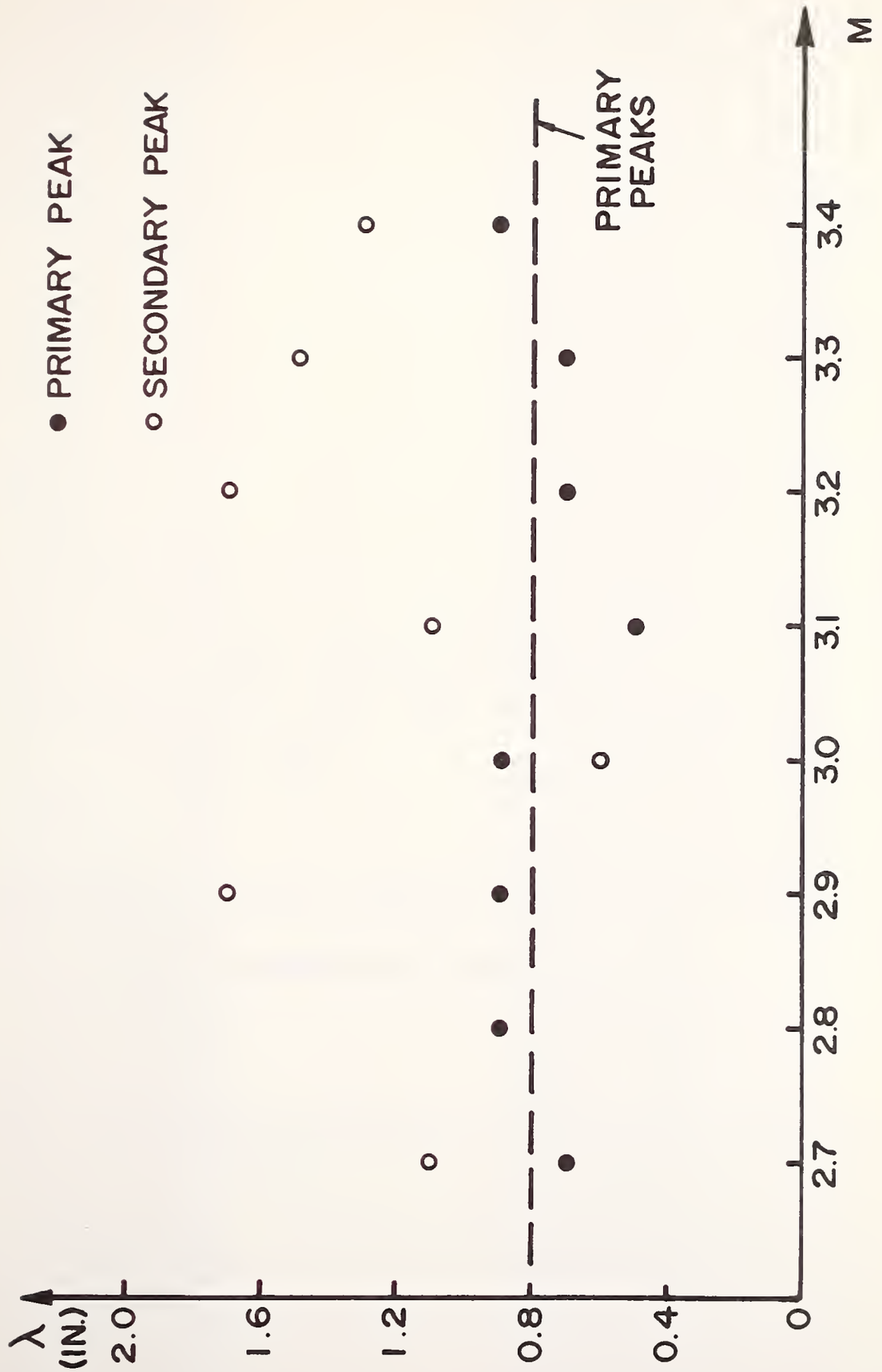

Figure 19. Disturbance Spectra Peaks Vs. Mach Number

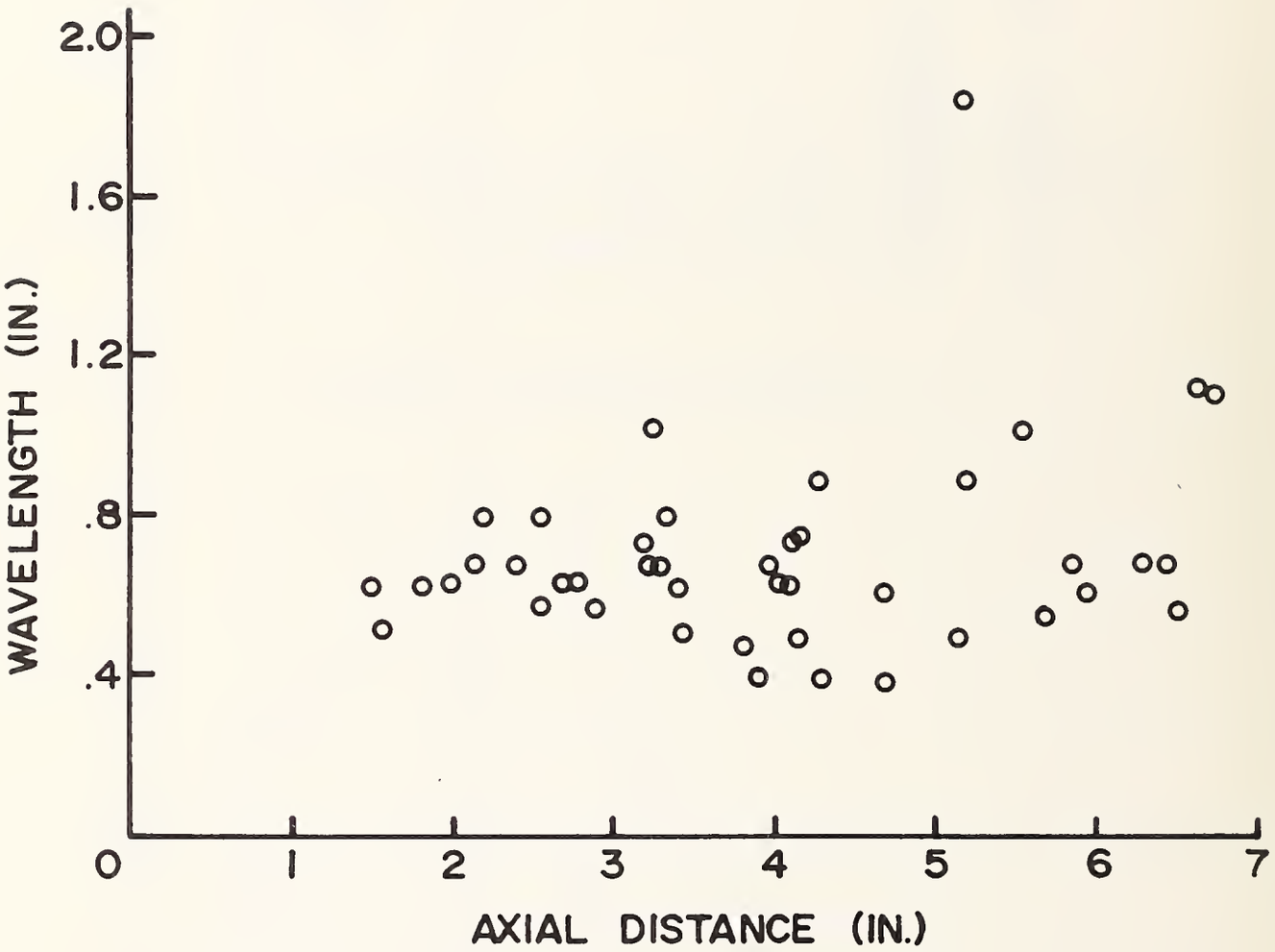

Figure 20. Axial Variation in Disturbance Wavelength, M = 2.7

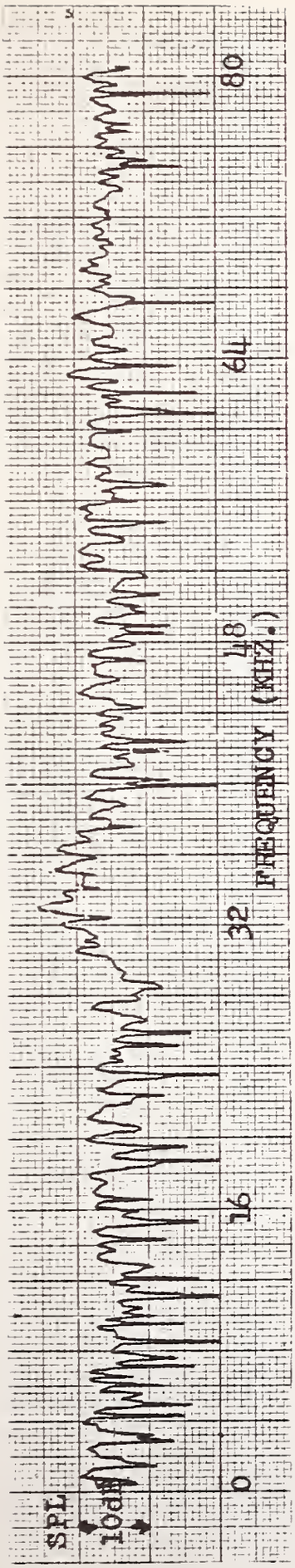

Figure 21. Acoustic Spectrum, M = 2.7

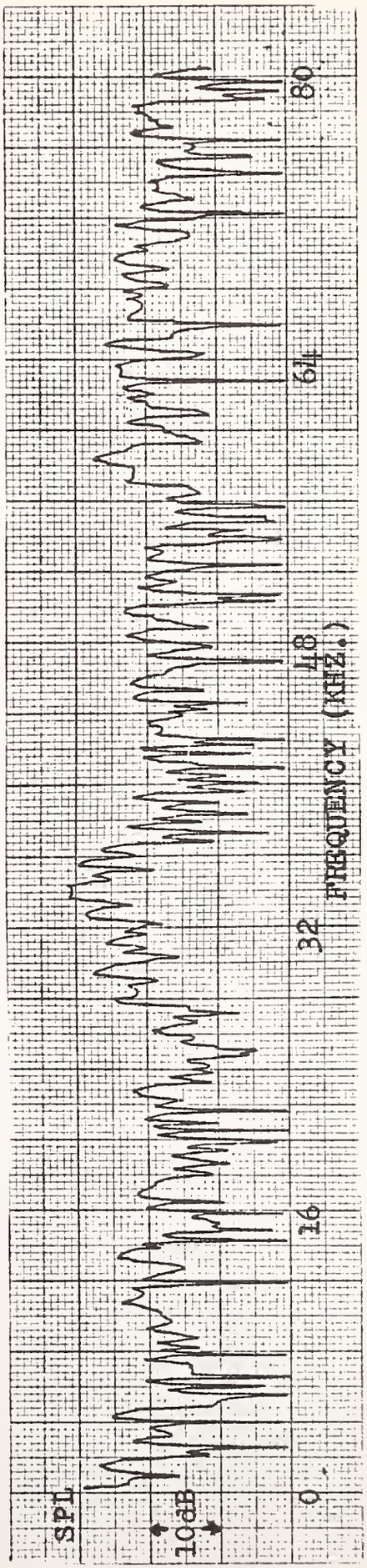

Figure 22. Acoustic Spectrum, M = 2.8

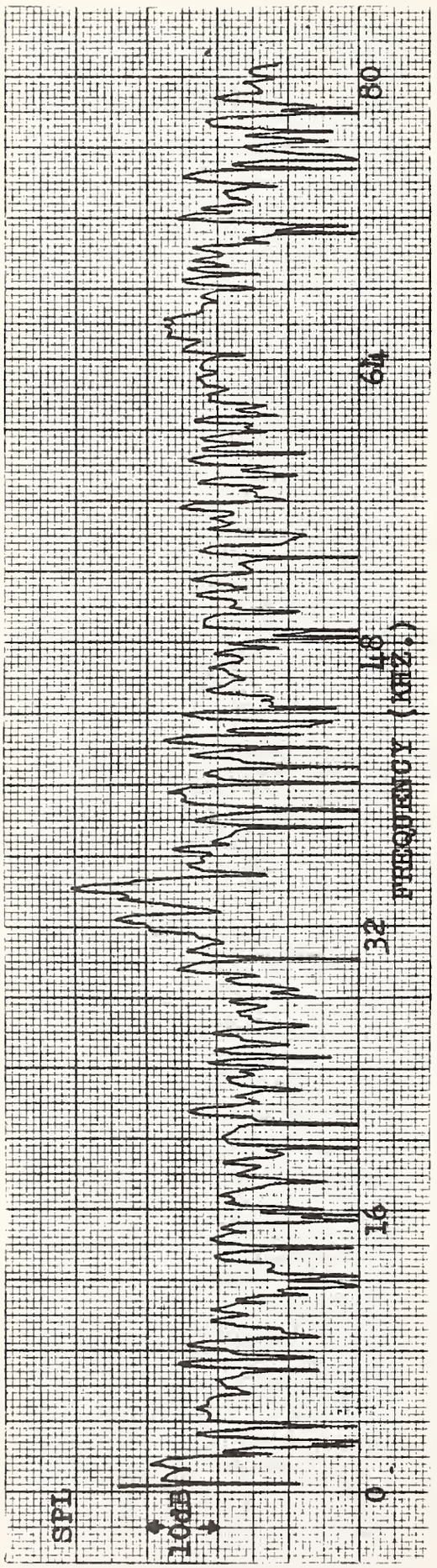

Figure 23. Acoustic Spectrum, M = 3.0

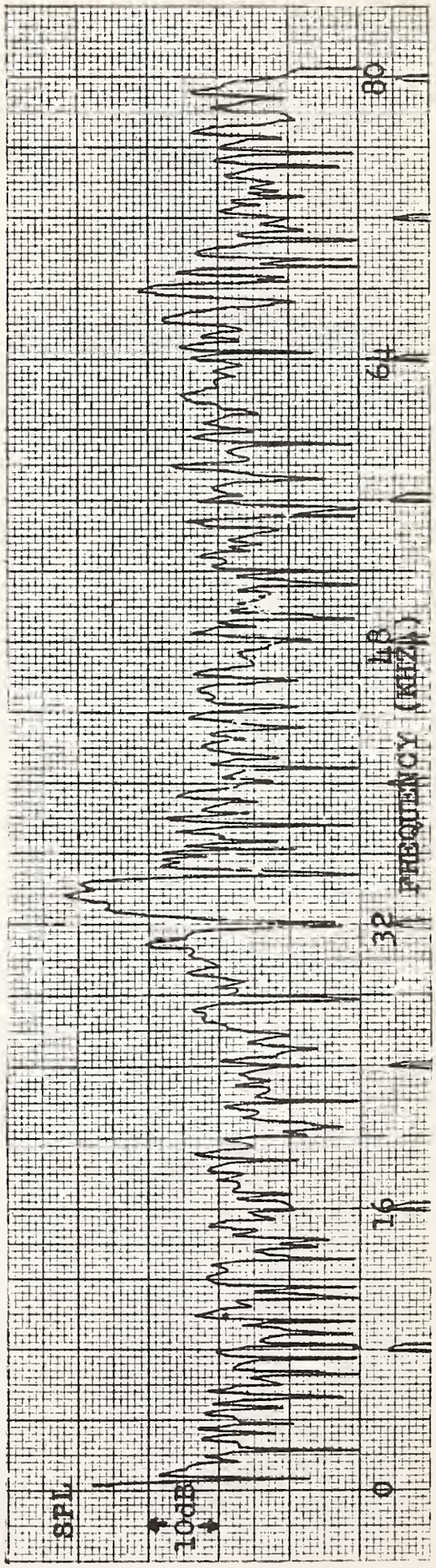

Figure 24. Acoustic Spectrum, M = 3.1

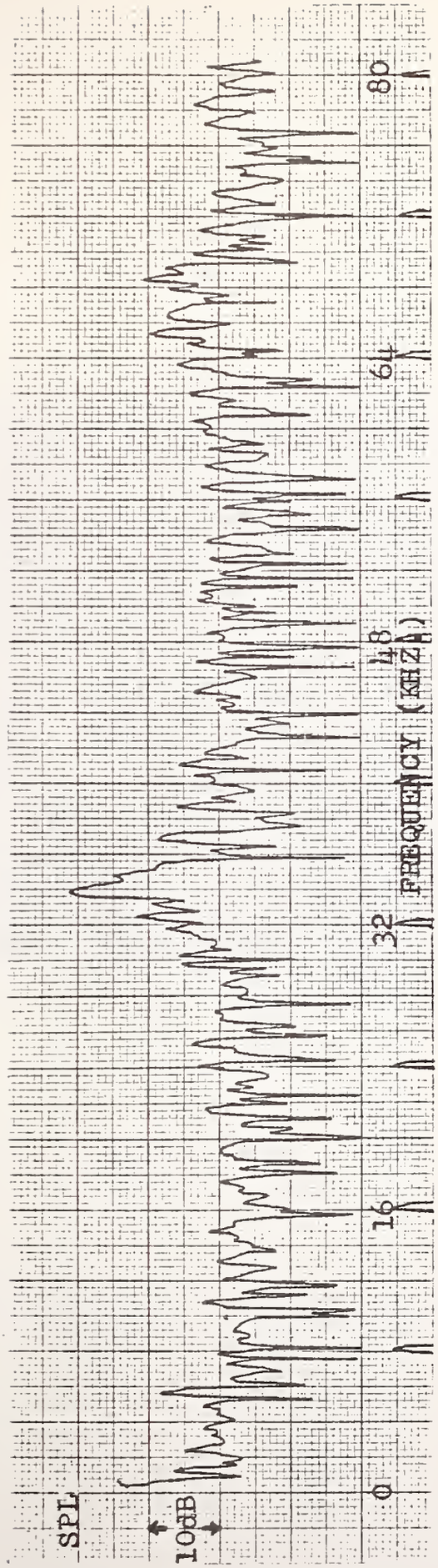

Figure 25. Acoustic Spectrum, M = 3.2

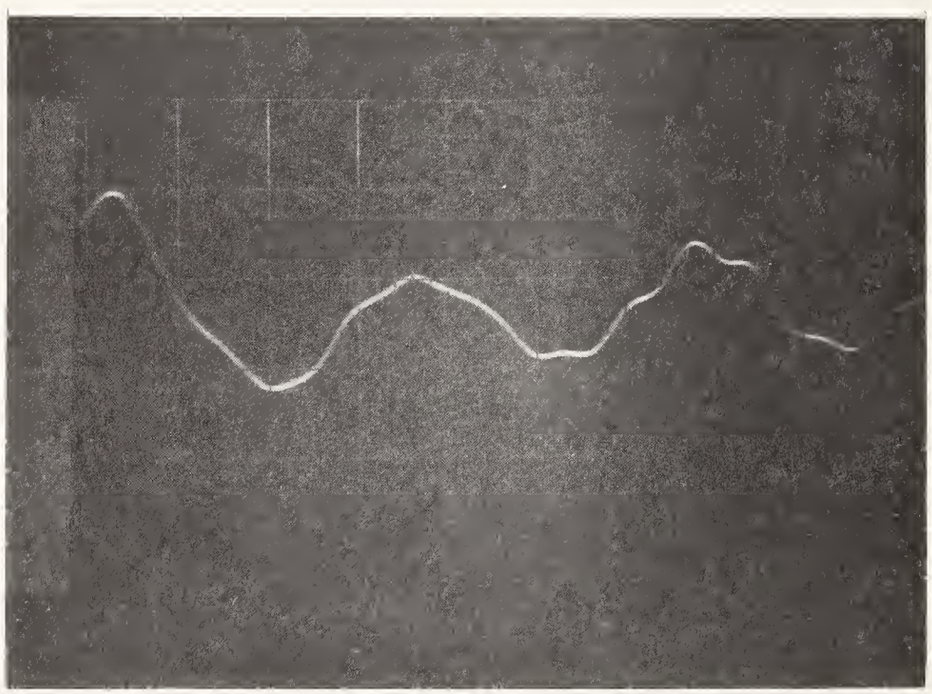

Horizontal Scale: 10 μsec./div.

Vertical Scale: 33.3 g./div.

Figure 26. Accelerometer Measurement of Nozzle Vibrations